Signals for gauge-mediated supersymmetry-breaking models at the CERN LEP 2 collider

S. Ambrosanio,* Graham D. Kribs,† and Stephen P. Martin‡

Randall Physics Laboratory, University of Michigan, Ann Arbor, Michigan 48109-1120

We consider a general class of models with gauge-mediated supersymmetry breaking in which the gravitino is the lightest supersymmetric particle. Several qualitatively different scenarios arise for the phenomenology of such models, depending on which superpartner(s) decay dominantly to the gravitino. At CERN LEP 2, neutralino pair production and slepton pair production can lead to a variety of promising discovery signals, which we systematically study. We investigate the impact of backgrounds for these signals and show how they can be reduced, and outline the effects of model parameter variations on the discovery potential. [S0556-2821(97)02815-4]

PACS number(s): 14.80.Ly, 12.60.Jv

I. INTRODUCTION

Low-energy supersymmetry (SUSY) can provide a natural solution to the hierarchy problem associated with the ratio M_Z/M_{Planck}. If nature is indeed supersymmetric, it is important to understand the mechanism by which SUSY breaking occurs and is transmitted to the particles of the standard model and their superpartners. One possibility is that SUSY is broken at a scale $\sim 10^{11}$ GeV in a sector which communicates with the particles of the minimal supersymmetric standard model (MSSM) only through gravitational interactions. This has historically been the most popular approach, and its phenomenological consequences have been and continue to be well studied. In this paper, we will be concerned instead with a different class of "gauge-mediated SUSY-breaking" (GMSB) models, in which the messengers of supersymmetry breaking are the ordinary gauge interactions [1,2].

Because gauge interactions are flavor blind, GMSB models are highly predictive with respect to the form of soft SUSY-breaking interactions. In the minimal model of GMSB [2], the squark, slepton, neutralino, and chargino masses are determined by only a handful of free parameters. The MSSM gaugino mass parameters necessarily have a common complex phase, which can be rotated away. Squarks and sleptons with the same electroweak quantum numbers are automatically degenerate in mass, up to radiative corrections involving Yukawa couplings which can be safely neglected for the sfermions of the first two families. Thus GMSB models have the pleasant feature that they are automatically free of excessive non-standard-model flavor-changing neutral currents; this also holds in a large class of extensions and variations of the minimal model [3–23]. Furthermore, the sparticle mass pattern is highly constrained even in extensions of the minimal model which contain many more parameters. This means that sparticle spectroscopy may one day provide for critical tests of GMSB.

However, the most distinctive phenomenological feature of GMSB models may be that, unlike in gravity-mediated

SUSY-breaking models, the gravitino ($\widetilde{G}$) is generally the lightest supersymmetric particle (LSP). This is because the scale $\sqrt{F}$ associated with dynamical SUSY breakdown can be as low as 10 TeV. The spin-$\frac{3}{2}$ gravitino obtains its mass by the super-Higgs mechanism, absorbing the spin-$\frac{1}{2}$ would-be Goldstino which couples to the divergence of the supercurrent with strength $1/F$. The resulting gravitino mass is

$$m_{\widetilde{G}} = \frac{F}{\sqrt{3}M} = 2.37 \times 10^{-2} \left(\frac{\sqrt{F}}{10 \text{ TeV}} \right)^2 \text{ eV}, \qquad (1)$$

where $M = (8\pi G_{\text{Newton}})^{-1/2} = 2.4 \times 10^{18}$ GeV. The next-to-lightest supersymmetric particle (NLSP) can therefore decay into its standard model partner and a gravitino [24–26]. (In this paper we assume exact R-parity conservation, so that there are no competing decays available for the NSLP.) If the scale $\sqrt{F}$ does not exceed a few thousand TeV, the decays can occur within a collider detector volume, possibly with a measurable decay length. Furthermore, even supersymmetric particles which are not the NLSP can decay into their standard model partners and a gravitino, if no competing decays are kinematically allowed. As we will see below, this may be an important consideration. The perhaps surprising relevance of a light gravitino for collider physics [24–37] can be traced to the fact that the interactions of the longitudinal components of the gravitino are the same as that of the Goldstino it has absorbed, and are proportional to $1/m_{\widetilde{G}}^2$ (or equivalently to $1/F^2$) in the light gravitino (small F) limit [24].

In the GMSB models to be considered in this study, the NLSP is always either a neutralino or a charged slepton. In the former case, the lightest neutralino ($\widetilde{N}_1$) decays into a photon and a gravitino with a width

$$\Gamma(\widetilde{N}_1 \rightarrow \gamma\widetilde{G}) = \frac{\kappa_{1\gamma}}{48\pi} \frac{m_{\widetilde{N}_1}^5}{M^2 m_{\widetilde{G}}^2}$$

$$= 20\kappa_{1\gamma} \left(\frac{m_{\widetilde{N}_1}}{100 \text{ GeV}} \right)^5 \left(\frac{\sqrt{F}}{10 \text{ TeV}} \right)^{-4} \text{ eV}, \qquad (2)$$

*Electronic address: ambros@umich.edu
†Electronic address: kribs@umich.edu
‡Electronic address: spmartin@umich.edu

where $\kappa_{1\gamma}=|N_{11}\cos\theta_W+N_{12}\sin\theta_W|^2$ is the photino component of $\widetilde{N}_1$ (using the notation of [38] for the neutralino mixing matrices N_{ij}). The probability that an $\widetilde{N}_1$ with energy E in the lab frame will decay before traveling a distance x is then

$$P(x)=1-e^{-x/L}, \qquad (3)$$

where

$$L=9.9\times10^{-7}\ \frac{1}{\kappa_{1\gamma}}\left(\frac{m_{\widetilde{N}_1}}{100\ \mathrm{GeV}}\right)^{-5}\left(\frac{\sqrt{F}}{10\ \mathrm{TeV}}\right)^4$$
$$\times(E_{\widetilde{N}_1}^2/m_{\widetilde{N}_1}^2-1)^{1/2}\ \mathrm{cm}. \qquad (4)$$

In principle, one can also have $\widetilde{N}_1\to Z\widetilde{G}$ or $h\widetilde{G}$, but the corresponding decay widths [30] suffer a strong kinematic suppression and can easily be shown to be always negligible within the context of the present paper.

In the rest frame of the decaying $\widetilde{N}_1$, the photon is produced isotropically (independent of the spin of $\widetilde{N}_1$) with energy equal to $m_{\widetilde{N}_1}/2$. The gravitino still escapes the detector, carrying away missing energy. Therefore SUSY discovery signals at colliders involve up to two energetic photons and missing (transverse) energy in GMSB models with a neutralino NLSP [24–36]. At the Tevatron, the largest production cross sections typically involve chargino ($\widetilde{C}_i$) and neutralino ($\widetilde{N}_i$) production, especially $p\bar{p}\to\widetilde{C}_1^+\widetilde{C}_1^-$ and $\widetilde{C}_1^\pm\widetilde{N}_2$. One can therefore detect supersymmetry using an inclusive $\gamma\gamma+\not{E}_T+X$ signal, in addition to channels with lepton(s)+jet(s)+0 or 1 photon. The discovery signatures for SUSY with a prompt decay $\widetilde{N}_1\to\gamma\widetilde{G}$ are so spectacular that it is possible to set quite significant bounds even with existing Fermilab Tevatron data. For example, in [30] it was argued that with the present ~100 pb^{-1} of Fermilab Tevatron data, it should be possible to exclude chargino masses up to about 125 GeV and neutralino masses up to about 70 GeV in a large class of models with a light gravitino, including GMSB models, as long as the decay $\widetilde{N}_1\to\gamma\widetilde{G}$ occurs within the detector.[1] In Ref. [35], a significant reach was found also in the 0 and 1 photon channels.

In discussing exclusion possibilities at the Tevatron, we must mention that a single unusual event [39] of this general type has been observed at the Collider Detector at Fermilab (CDF). This event has large (>50 GeV) $\not{E}_T$ and two central ($|\eta|<1$), energetic ($E_T>30$ GeV) photons and two energetic leptons. Events with these characteristics are reputed to have very small standard model and detector backgrounds, and it was pointed out in [26,28] that this event might be explained by GMSB models (and other models with a light gravitino) in terms of selectron pair production. However, at least in the simplest types of GMSB models, this interpretation is now perhaps somewhat disfavored, since one might typically expect many accompanying events in other chan-

nels [29–31,35], which have not turned up in recent searches by (CDF) [40] and by D0 [41] Collaborations. Perhaps a more plausible explanation of the event within the GMSB framework is that it was due to chargino pair production $p\bar{p}\to\widetilde{C}_1^+\widetilde{C}_1^-$, as proposed in [30,31]. Each of the charginos can decay either hadronically into $q\bar{q}'\gamma\widetilde{G}$ or leptonically into $l\nu\gamma\widetilde{G}$. The latter possibility can be significantly enhanced if sneutrinos are not too heavy (although it still seems somewhat problematic to explain the kinematics of the observed event). GMSB models can be constructed with a neutralino NLSP and a large leptonic branching fraction for $\widetilde{C}_1$ (with $m_{\widetilde{C}_1}>m_{\widetilde{\nu}}$), but not with a minimal messenger sector. The signal for $\widetilde{C}_1^+\widetilde{C}_1^-$ production in this case can then be $l^+l'^-\gamma\gamma\not{E}_T$. Note that in this chargino interpretation of the event, the leptons need not have the same flavor. In any case, more data at the Tevatron and at CERN LEP 2 will help to test these speculations.

In other GMSB models, one finds that the NLSP is a stau. Here, one should distinguish between several qualitatively distinct situations. If $\tan\beta$ (the ratio of Higgs expectation values $\langle H_u^0\rangle/\langle H_d^0\rangle$) is not too large, the lightest stau eigenstate $\widetilde{\tau}_1$ is predominantly right handed and is nearly degenerate in mass with the other right-handed sleptons. In the case that $m_{\widetilde{e}_R}\approx m_{\widetilde{\mu}_R}<m_{\widetilde{\tau}_1}+m_\tau$, one finds that the $\widetilde{e}_R$ and $\widetilde{\mu}_R$ cannot have three-body decays into $\widetilde{\tau}_1$ without violating lepton flavor conservation. Since lepton flavor-changing interactions are automatically very highly suppressed in GMSB models with R-parity conservation and decays through an off-shell tau are insignificant, each of the right-handed sleptons decays only into the corresponding lepton+gravitino [26], and $\widetilde{\tau}_1,\widetilde{\mu}_R,\widetilde{e}_R$ act effectively as co-NLSP's. (An exception occurs if $m_{\widetilde{\tau}_1}<m_{\widetilde{N}_1}<m_{\widetilde{e}_R}$, as discussed below.) In this case, all supersymmetric decay chains will terminate in $\widetilde{\tau}_1\to\tau\widetilde{G}$ or $\widetilde{e}_R\to e\widetilde{G}$ or $\widetilde{\mu}_R\to\mu\widetilde{G}$. The formulas for the relevant decay widths of slepton into lepton+gravitino are given by simply replacing $m_{\widetilde{N}_1}\to m_{\widetilde{l}}$, $E_{\widetilde{N}_1}\to E_{\widetilde{l}}$ and $\kappa_{1\gamma}\to1$ in Eqs. (2) and (4), so that the decay length in the lab frame for a slepton with energy $E_{\widetilde{l}}$ is

$$L=9.9\times10^{-7}\left(\frac{m_{\widetilde{l}}}{100\ \mathrm{GeV}}\right)^{-5}\left(\frac{\sqrt{F}}{10\ \mathrm{TeV}}\right)^4$$
$$\times(E_{\widetilde{l}}^2/m_{\widetilde{l}}^2-1)^{1/2}\ \mathrm{cm}. \qquad (5)$$

At LEP 2 energies, the primary discovery process often (but certainly not always, as we shall see) involves simple pair production of the NLSP. In that case, $E_{\widetilde{N}_1}$ in Eq. (4) and $E_{\widetilde{l}}$ in Eq. (5) can simply be replaced by the electron beam energy at LEP 2.

Conversely, if $\widetilde{\tau}_1$ is the NLSP and $\tan\beta$ exceeds 4 to 8 (depending on the other model parameters), one finds in GMSB models that $m_{\widetilde{\tau}_1}$ is small enough that the decays $\widetilde{l}_R\to\widetilde{\tau}_1\tau l$ are kinematically allowed for $l=e,\mu$. These three-body decays are mediated by virtual neutralinos and are typically not dynamically suppressed, because the bino content of $\widetilde{N}_1$ is significant. However, we have checked that they can be quite strongly suppressed by phase space, so that it is possible for $\widetilde{l}_R\to l\widetilde{G}$ to dominate even if $m_{\widetilde{l}_R}-m_{\widetilde{\tau}_1}-m_\tau$

---

[1] A quite similar bound on $m_{\widetilde{N}_1}$ in a large class of GMSB models may be obtained using the recent CERN e^+e^- collider LEP runs at $\sqrt{s}=161,172$ GeV, as we will see in Sec. III.

$-m_l$ is a few GeV, if $\sqrt{F}$ is not too large and $\widetilde{l}_R \rightarrow l\widetilde{N}_1$ is kinematically disallowed. Barring these circumstances, $\widetilde{\tau}_1$ acts as the sole NLSP, and all supersymmetric decay chains will terminate in $\widetilde{\tau}_1 \rightarrow \tau\widetilde{G}$ [34].

An important exception to the preceding discussion occurs if $|m_{\widetilde{N}_1} - m_{\widetilde{\tau}_1}| < m_\tau$ and $m_{\widetilde{N}_1} < m_{\widetilde{l}_R} + m_l$ for $l = e, \mu$. Then each of the decays $\widetilde{N}_1 \rightarrow \gamma\widetilde{G}$ and $\widetilde{\tau}_1 \rightarrow \tau\widetilde{G}$ have no significant competition, and $\widetilde{N}_1$ and $\widetilde{\tau}_1$ act effectively as co-NLSP's.

To summarize, there are four qualitatively distinct scenarios for the termination of supersymmetric decay chains in GMSB models. By a slight abuse of language, we refer to these as ''neutralino NLSP,'' ''stau NLSP,'' ''slepton co-NLSP,'' and ''neutralino-stau co-NLSP'' scenarios, according to whether A only, B only, B and C, or A and B of the decays

$$(A) \quad \widetilde{N}_1 \rightarrow \gamma\widetilde{G}, \tag{6}$$

$$(B) \quad \widetilde{\tau}_1 \rightarrow \tau\widetilde{G}, \tag{7}$$

$$(C) \quad \widetilde{l}_R \rightarrow l\widetilde{G} \quad (l = e, \mu), \tag{8}$$

do not suffer competition. The four possible scenarios correspond nominally to the mass orderings (in addition to $m_{\widetilde{\tau}_1} < m_{\widetilde{l}_R}$ for $l = e, \mu$, which turns out to be always satisfied in the GMSB parameter space we consider):

$$\text{neutralino NLSP:} \quad m_{\widetilde{N}_1} < m_{\widetilde{\tau}_1} - m_\tau, \tag{9}$$

$$\text{stau NLSP:} \quad m_{\widetilde{\tau}_1} < \min[m_{\widetilde{N}_1}, m_{\widetilde{l}_R}] - m_\tau, \tag{10}$$

$$\text{slepton co-NLSP:} \quad m_{\widetilde{l}_R} < \min[m_{\widetilde{N}_1}, m_{\widetilde{\tau}_1} + m_\tau], \tag{11}$$

$$\text{neutralino-stau-co-NLSP:} \quad |m_{\widetilde{\tau}_1} - m_{\widetilde{N}_1}| < m_\tau; \quad m_{\widetilde{N}_1} < m_{\widetilde{l}_R}, \tag{12}$$

where we have neglected the masses of the electron and the muon. We should note that the condition Eq. (10) for the stau NLSP scenario is necessary but not quite sufficient, since as we have already noted, the decay $\widetilde{l}_R \rightarrow l\widetilde{G}$ can dominate over $\widetilde{l}_R \rightarrow \widetilde{\tau}_1 \tau l$ when the latter is kinematically open but suppressed. Thus some models which obey Eq. (10) may actually behave as slepton co-NLSP models, depending on $\sqrt{F}$. We have checked that two-body decays $\widetilde{l} \rightarrow l\widetilde{N}_1$ always dominate over decays into the gravitino as long as $\sqrt{F} > 10$ TeV and the mass difference $m_{\widetilde{l}} - m_{\widetilde{N}_1} - m_l$ is more than of order 10 MeV for $l = e$ (and much less for $l = \mu, \tau$). A similar statement holds for two-body decays $\widetilde{N}_1 \rightarrow l\widetilde{l}$. Hence we will consider only the four main scenarios listed above. Other ''borderline'' cases with small mass differences will have similar phenomenology to the cases we do treat.

In Sec. II of this paper we describe the framework for an exploration of the parameter space of GMSB models, with some simplifying but hopefully not overly restrictive assumptions. In Sec. III, we give some conditions on the parameters for each of the four different NLSP scenarios, and study the possible signals and backgrounds which arise at

LEP 2 in each case. We will mostly consider an option with $\sqrt{s} = 190$ GeV and 300 pb^{-1} per detector. Section IV contains some concluding remarks.

II. MODELS OF GAUGE-MEDIATED SUSY BREAKING

In this paper we will consider the following class of GMSB models. The ultimate source of SUSY breaking is parametrized by a gauge-singlet chiral superfield S whose scalar and auxiliary components are both assumed to acquire vacuum expectation values (VEV's), denoted S and F_S, respectively. The superfield S couples to a ''messenger sector'' consisting of chiral superfields $\Phi_i, \overline{\Phi}_i$ which transform as a vectorlike representation of $SU(3)_C \times SU(2)_L \times U(1)_Y$. The messenger sector couples to the SUSY-breaking sector through the superpotential

$$W = \lambda_i S \Phi_i \overline{\Phi}_i. \tag{13}$$

This implies that the fermionic messengers acquire a Dirac mass $\lambda_i S$, while their scalar partners obtain (mass)^2 $= |\lambda_i S|^2 \pm |\lambda_i F_S|$. The ordinary gauge interactions then transmit this SUSY violation to the MSSM fields, with computable superpartner masses [1,2]. Contributions to gaugino masses due to each messenger pair $\Phi_i, \overline{\Phi}_i$ arise at one loop and are given at the scale(s) $Q = \lambda_i S$ by

$$\Delta M_a = \frac{\alpha_a}{4\pi} \Lambda n_a(i) g(x_i) \quad (a = 1,2,3), \tag{14}$$

where

$$\Lambda \equiv F_S / S, \tag{15}$$

$$g(x) = \frac{1}{x^2} [(1+x)\ln(1+x) + (1-x)\ln(1-x)], \tag{16}$$

and each

$$x_i \equiv |F_S / \lambda_i S^2|. \tag{17}$$

The latter quantities must satisfy $0 < x_i < 1$ (so that the lightest messenger scalar does not acquire a VEV). Here $n_a(i)$ is the Dynkin index for the messenger pair $\Phi_i, \overline{\Phi}_i$ in a normalization where $n_a = 1$ for $\mathbf{N} + \overline{\mathbf{N}}$ of $SU(N)$. We always use a grand unified theory (GUT) normalization for α_1 so that $n_1 = \frac{6}{5}Y^2$ for each messenger pair with weak hypercharge $Y = Q_{EM} - T_3$. In the limit of small x_i and when $\Phi_i, \overline{\Phi}_i$ consist of a $\mathbf{5} + \overline{\mathbf{5}}$ of the global $SU(5)$ which contains $SU(3)_C \times SU(2)_L \times U(1)_Y$, one recovers the results for the original minimal GMSB models with $\Sigma n_a = 1$ and small x_i [2], since $g(0) = 1$. The function $g(x)$ is always slightly greater than 1, but never exceeds 1.044 when $x < 0.5$, and reaches a maximum of 1.386 at $x = 1$ [8].

Contributions from each messenger pair $\Phi_i, \overline{\Phi}_i$ to the (mass)^2 terms of the MSSM scalars arise at two-loop order and are given at the scale(s) $Q = \lambda_i S$ by

$$\Delta\widetilde{m}^2 = 2\Lambda^2 \sum_a \left(\frac{\alpha_a}{4\pi}\right)^2 C_a n_a(i) f(x_i), \tag{18}$$

where [4]

$$f(x) = \frac{1+x}{x^2} \left[\ln(1+x) - 2 \text{Li}_2(x/[1+x]) \right. $$
$$\left. + \frac{1}{2} \text{Li}_2(2x/[1+x]) \right] + (x \rightarrow -x) \qquad (19)$$

and C_a is the quadratic Casimir invariant of the MSSM scalar field in question, in a normalization where $C_3 = \frac{4}{3}$ for color triplets, $C_2 = \frac{3}{4}$ for $SU(2)_L$ doublets, and $C_1 = \frac{3}{5} Y^2$. For small x_i, one has $f(x_i) \approx 1$, so that again the results of the original minimal model with small x_i [2] are recovered.

In order to have a manageable parameter space for our study, we now make some simplifying assumptions. First, we consider (except when explicitly noted) only models for which the total Dynkin indices of the messenger sector for each gauge group are equal and do not exceed 4:

$$n = \sum_i n_1(i) = \sum_i n_2(i) = \sum_i n_3(i) = 1,2,3, \text{ or } 4. \qquad (20)$$

This assumption ensures that the apparent near unification of perturbative gauge couplings near $M_U \approx 2 \times 10^{16}$ GeV is maintained. (Possibilities which do not embrace this assumption are discussed in [8].) We will also take all of the couplings λ_i to be equal to a common value λ, even though no symmetry can enforce this; variations in the individual λ_i only affect the MSSM sparticle spectrum logarithmically. This in turn forces all of the x_i to be equal to a single parameter x, which as a practical matter we require to satisfy

$$0.01 < x < 0.9. \qquad (21)$$

With these assumptions, MSSM phenomenology is determined by just six parameters:

$$\Lambda, n, x, \lambda, \tan\beta, \quad \text{and } \text{sgn}(\mu). \qquad (22)$$

The expressions for the sum of contributions to gaugino and sfermion masses now simplify to

$$M_a = n \Lambda g(x) \frac{\alpha_a}{4\pi}, \qquad (23)$$

$$\widetilde{m}^2 = 2n \Lambda^2 f(x) \sum_a \left(\frac{\alpha_a}{4\pi} \right)^2 C_a \qquad (24)$$

at the single messenger scale $Q_{\text{mess}} = \Lambda/x$. Equations (23) and (24) are taken as boundary conditions for renormalization group (RG) evolution of the MSSM parameters. At the same scale Q_{mess}, the running trilinear scalar couplings of the MSSM are taken to vanish (they actually receive contributions at two-loop order which are negligible in the first approximation). However, we do not assume that $B\mu$ is close to zero at the messenger scale, since it seems likely that a mechanism for generating μ can also generate $B\mu$ [2,3,6]. We then evolve all of the couplings of the MSSM from Q_{mess} down to the electroweak scale, where the parameters $B\mu$ and $|\mu|$ are determined by requiring correct electroweak symmetry breaking. Note that in this parametrization, the

sparticle spectrum (with the exception of the gravitino mass) does not depend on λ, and depends on x only logarithmically through Q_{mess} and $g(x)$. Of course, allowing different x_i, λ_i would be more realistic and would enlarge the parameter space. However, the features of the enlarged parameter space obtained in this way do not differ dramatically from the one we consider. The effect of finite x_i in Eqs. (14) and (18) is simply to raise the gaugino mass parameters by up to about 25% with respect to the sfermion masses, since $g(x)/\sqrt{f(x)}$ varies between 1 (for $x \ll 1$) and 1.25 (for $x = 0.9$). Choosing a specific value of x can be thought of as simply parametrizing our ignorance of these effects within a simplified framework. In the present paper, the chargino, squark, and gluino masses have no direct relevance, so that the practical effect of increasing x is essentially just to lower the slepton masses compared to the mass of the lightest neutralino.

The Goldstino decay constant in this parametrization is given by

$$F_S = \frac{\Lambda^2}{x_i \lambda_i} = \frac{\Lambda^2}{x\lambda}. \qquad (25)$$

This way of expressing F_S is useful because Λ is relatively well known from Eqs. (23) and (24), since it is correlated strongly with the mass of the NLSP which we must presume lies in the 50 to 100 GeV range in order for SUSY to be relevant at LEP 2. An easy estimate then shows that the relevant range of Λ for this paper is from about 10 to about 100 TeV. While the dimensionless couplings x and λ can be arbitrarily small, they can be bounded from above. Furthermore, F_S can be smaller than the full SUSY-breaking order parameter F of the complete theory. (In models where F_S arises directly from an O'Raifeartaigh mechanism one expects $F_S = F$, but in models where F_S itself arises radiatively as in [2], one may find $F_S \ll F$.) Therefore, Eq. (25) puts a lower limit on F, or equivalently a lower limit on $m_{\widetilde{G}}$, corresponding to a lower limit on the decay length of the NLSP according to Eqs. (4) and (5). In particular, we note that in viable GMSB models one must have

$$m_{\widetilde{G}} \gtrsim 2 \times 10^{-2} \text{ eV}, \qquad (26)$$

based only on $\lambda_i \lesssim 1$ and $m_{\text{NSLP}} > 50$ GeV; this is consistent with cosmological bounds [42] on $m_{\widetilde{G}}$. For any given sparticle spectrum specified by the parameters Λ, n, x, $\tan\beta$, $\text{sgn}(\mu)$, one obtains a lower limit on the NLSP decay length by assuming $\lambda \lesssim 1$. By taking smaller λ with Λ and x held constant one can essentially arbitrarily increase the NLSP decay length while holding all other features of the MSSM sparticle spectrum fixed. The NLSP decay length will also be increased if $F_S < F$, as long as a pseudo-Goldstino field which is not absorbed by the gravitino (and which is predominantly the fermionic component of S) acquires a large mass. In these cases the NLSP decay length L can be made so large that NLSP decays always occur outside the detector.

The statement that λ, or more generally the distinct couplings λ_i, should be bounded from above can be motivated as follows. An estimate of the maximum value of the cou-

plings λ_i should roughly correspond to an infrared quasifixed point of the RG equations. Let us consider, for example, a ''minimal'' messenger sector in which Φ_i, $\bar{\Phi}_i$ consist of a $5+\bar{5}$ of the global SU(5) group which contains the MSSM gauge group. In that case one has couplings λ_2 and λ_3 of S to the SU(2)$_L$-doublet and SU(3)$_C$-triplet messenger fields, respectively. These couplings satisfy the one-loop RG equations

$$16\pi^2 \frac{d\lambda_2}{dt} = \lambda_2\left[4\lambda_2^2 + 3\lambda_3^2 + \cdots - 3g_2^2 - \frac{3}{5}g_1^2\right], \quad (27)$$

$$16\pi^2 \frac{d\lambda_3}{dt} = \lambda_3\left[2\lambda_2^2 + 5\lambda_3^2 + \cdots - \frac{16}{3}g_3^2 - \frac{4}{15}g_1^2\right]. \quad (28)$$

Here the ellipses represent the effects of other dimensionless couplings involving S, Φ_i, or $\bar{\Phi}_i$. These are of course highly model dependent but will contribute positively to the one-loop β functions, thus only reducing the quasifixed point values of the couplings. One can then estimate the maximum quasifixed point values for (λ_2, λ_3) by taking $\lambda_3 = \lambda_2 = \lambda_U$ to be large at the putative unification scale and evolving down to the messenger scale. For example if the messenger scale is $Q_{\text{mess}} = 100$ TeV, then taking $\lambda_U \gtrsim 2$ yields $(\lambda_2, \lambda_3) \approx (0.7, 1.1)$ at Q_{mess}. Even if we abandon GUT boundary conditions in this example and choose $\lambda_3 \ll \lambda_2$ or $\lambda_2 \ll \lambda_3$ at the ''unification'' scale, the maximum values at the messenger scale of the dominant coupling are found to be $\lambda_2 \approx 1.0$ or $\lambda_3 \approx 1.2$, respectively. Of course, S need not be a fundamental chiral superfield, but the fixed point values for λ_i should roughly correspond to the maximum values, at least in a perturbative effective field theory description. Note that models with more messenger fields should respect the rough result $\lambda_i \lesssim 1$. Adding more couplings to the mix will effectively only give positive contributions to the corresponding β functions when compared with the example given above, leading to smaller values for the λ_i at the messenger scale. A larger messenger sector will cause the gauge couplings to be larger above the messenger scale, indirectly resulting in a decrease in the β functions for the λ_i. However, this can only slightly increase the quasifixed point behavior of the largest coupling(s), which is determined predominantly by what happens near the messenger scale. Therefore we expect that the lower bound on the NLSP decay length at LEP to be inferred from $\lambda \lesssim 1$ (for a given x) should be robust. In particular, we see from Eq. (25) that for models with a given Λ, the minimum possible decay length L for the NLSP is given by replacing $\sqrt{F} \to \Lambda$ in Eqs. (4) or (5).

In order to understand the parameter space of the GMSB models we have chosen to study, we have used a computer program to generate several tens of thousands of models for each of $n = 1, 2, 3, 4$ and random values for the other free parameters in Eq. (22). The program proceeds by an iterative method that sets the weak-scale gauge couplings and masses, evolves the RG equations to the messenger scale, sets the messenger scale boundary conditions, evolves the RG equations with associated decouplings at each sparticle threshold back to the weak scale, then iterates to convergence (about four iterations are typically necessary). Two-loop RG equa-

tions are used for the gauge couplings, third generation Yukawa couplings, and gaugino soft masses, while one-loop RG equations are used for the other soft masses and scalar trilinear couplings. Electroweak symmetry breaking is enforced at the scale $Q = \sqrt{m_{\tilde{t}_1} m_{\tilde{t}_2}}$, allowing the evaluation of $|\mu|$ and $B\mu$ from the Higgs soft masses, $\tan\beta$, M_Z, and one-loop corrections. This evaluation utilizes the one-loop effective potential, which includes the corrections from top squarks, bottom squarks, and staus consistently with the one-loop evaluation of the Higgs boson masses.

Because this paper is devoted to possible discovery signals at LEP 2, we consider only models with NLSP mass less than 100 GeV. The lightest supersymmetric particle is always a neutralino or a stau throughout this parameter space.[2] However, as explained in the Introduction, more than one superpartner can act effectively as the NLSP. We find significant regions of parameter space in which each of the four scenarios is indeed realized. In the next section we will describe in turn some relevant features of the parameter space, including conditions on the parameters n, Λ, and $\tan\beta$, for the four NLSP scenarios. In each case we study how the SUSY discovery signals may manifest themselves at LEP 2.

III. SIGNALS AT THE CERN LEP 2 COLLIDER

A. The neutralino NLSP scenario

If Eq. (9) is satisfied, then the lightest neutralino is the NLSP, and essentially all supersymmetric decay chains will terminate in $\tilde{N}_1 \to \gamma\tilde{G}$. If this decay always occurs outside of the detector, then collider signatures and search strategies are the same as in the well-studied neutralino LSP scenario (see for example [43,44]). In that case, the only impact of the gauge-mediation mechanism for collider phenomenology is that the pattern of supersymmetric masses and other soft supersymmetry breaking parameters is restricted in significant ways.

If the decay $\tilde{N}_1 \to \gamma\tilde{G}$ occurs within the detector an appreciable fraction of the time, then $\tilde{N}_1\tilde{N}_1$ production can lead to a discovery signal at LEP 2. A crucial quantity is then the decay length L in Eq. (4) with $E = \sqrt{s}/2$. For L greater than a few centimeters, the LEP detectors may be able to resolve the distance from the interaction point to the $\tilde{N}_1$ decay vertex where the photon originates. If this can be done reliably, there should be essentially no backgrounds to the signal. However, as L increases, a larger fraction of events will occur outside the detector, decreasing the efficiency accordingly. Of course, any analysis of this situation would be highly detector dependent, as the different LEP detectors have varying geometries and photon direction resolution capabilities. For a rough study we suppose that photons resulting from decays $\tilde{N}_1 \to \gamma\tilde{G}$ can be detected if they occur

---

[2]We find one exception: it is possible to construct models with $n = 3$ or 4 which have a tau sneutrino NLSP, but only if $m_{\tilde{\nu}_\tau} < 54$ GeV and $m_{\tilde{l}_R} < 57$ GeV and $m_{\tilde{l}_L} < 95$ GeV. We neglect this possibility in the following, although a complete analysis which might exclude these models has not yet been performed to our knowledge.
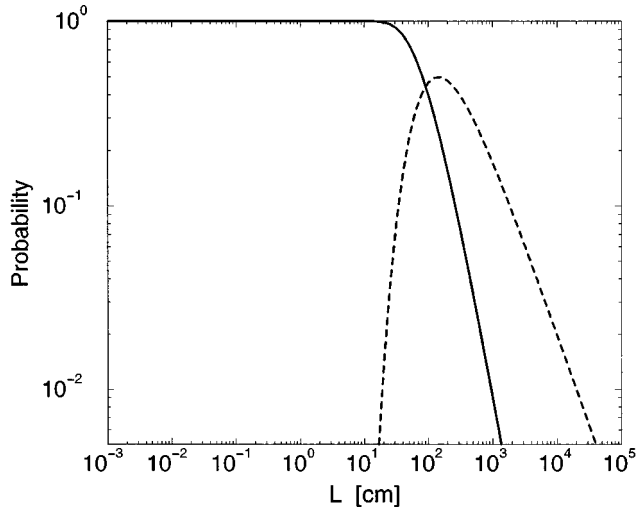
FIG. 1. The probability that exactly one (two) of the photons from the decay $\widetilde{N}_1 \rightarrow \gamma \widetilde{G}$ originates within 1 m of the $\widetilde{N}_1 \widetilde{N}_1$ production vertex is shown as the dashed (solid) curve, as a function of the decay length L.

within 1 m of the interaction point. Using Eqs. (3) and (4), we can then estimate, as a function of the parameter L, the probabilities that both, or only one, of the photons can be detected in each event. These probabilities are shown in Fig. 1 for 10^{-3} cm $< L < 10^5$ cm. (This range corresponds roughly to $1 \gtrsim x\lambda \gtrsim 10^{-4}$ for the models described in Sec. II with $m_{\widetilde{N}_1} < 90$ GeV and $\sqrt{s} = 190$ GeV.) Note that the probability to observe one of the two photons in each event may exceed 0.1 even for L greater than 10 m. Remarkably, an observable signal with displaced (not originating from the interaction point) single photons might occur for L up to several tens of m, depending on the $\widetilde{N}_1 \widetilde{N}_1$ production cross section (typically in the tens or hundreds of fb), the integrated luminosity achieved, and the specific detector being used. For L in the several cm to several m range, one can hope to observe both one photon and two photon events with displaced vertices.

For the remainder of this subsection, we assume that L is less than a few tens of cm, so that essentially all decays $\widetilde{N}_1 \rightarrow \gamma \widetilde{G}$ occur within the detector. We consider only models for which $m_{\widetilde{N}_1} < 100$ GeV (so that $\widetilde{N}_1 \widetilde{N}_1$ production can be possible at LEP 2) and $m_{\widetilde{N}_1} > 70$ GeV (motivated [30] by the nonobservation of excessive $\gamma\gamma + \not{E}_T + X$ events at the Tevatron [40,41]). Then we find that within the framework of GMSB models assumed here, neutralino NLSP models can only be constructed if

$$n = 1; \quad 40 \text{ TeV} < \Lambda < 80 \text{ TeV}; \quad \tan\beta < 35, \text{ or} \quad (29)$$

$$n = 2; \quad 24 \text{ TeV} < \Lambda < 40 \text{ TeV}; \quad \tan\beta < 18, \text{ or} \quad (30)$$

$$n = 3; \quad 20 \text{ TeV} < \Lambda < 24 \text{ TeV}; \quad \tan\beta < 10 \text{ and } \mu > 0. \quad (31)$$

These conditions are necessary, but not sufficient. The upper and lower bounds on Λ correspond to those on $m_{\widetilde{N}_1}$ in the obvious way. The upper limits on $\tan\beta$ follow from the requirement that $m_{\tau_1} > m_{\widetilde{N}_1} + m_\tau$; for larger values of $\tan\beta$ the

mixing in the stau (mass)^2 matrix becomes too large to allow this. In all cases, one finds that $|\mu| \gtrsim M_2$, so that the NLSP has a significant photino component, with $0.4 < \kappa_{1\gamma} < 0.85$ in all models of this type, and $\kappa_{1\gamma} > 0.55$ in the minimal model (meaning $n = 1$). We have verified that for all neutralino NLSP models accessible at LEP 2, the $B(\widetilde{N}_1 \rightarrow \gamma\widetilde{G})$ is in practice indistinguishable from 100%. In the models described above, the minimum possible decay length L [estimated by substituting $E_{\widetilde{N}_1} = \sqrt{s}/2$ and $\sqrt{F} \approx \Lambda$ in Eq. (4)] is typically of order 10 to 100 μm, far smaller than the resolution of the detectors.

Neutralinos can be pair produced in $e^+ e^-$ collisions by Z exchange in the s channel or by selectron exchange in the t channel. In GMSB models, $\widetilde{N}_1$ is always predominantly a bino and the ratio $m_{\widetilde{e}_R}/m_{\widetilde{N}_1}$ cannot be larger than (1.6,1.25,1.1) for $n = (1,2,3)$. Therefore the dominant contribution to $\widetilde{N}_1 \widetilde{N}_1$ production always comes from $\widetilde{e}_R$ exchange because of the relatively large $e - \widetilde{e}_R$-bino coupling. Indeed, the nonminimal GMSB models with $n = 2,3$ tend to have a larger cross section for $e^+ e^- \rightarrow \widetilde{N}_1 \widetilde{N}_1$ because of relatively lighter $m_{\widetilde{e}_R}$ for fixed $m_{\widetilde{N}_1}$. In addition, in some models $\widetilde{l}_R \widetilde{l}_R$ production (or just $\widetilde{\tau}_1 \widetilde{\tau}_1$) production is allowed at LEP 2. However, we find that in the neutralino NLSP scenario, the individual slepton production cross sections are always smaller by at least a factor of 2 (and often much more), so we will concentrate first on $\widetilde{N}_1 \widetilde{N}_1$ production as the discovery process. We also find that chargino pair production is never allowed at LEP 2, and $\widetilde{N}_1 \widetilde{N}_2$ is sometimes allowed but is always highly kinematically suppressed and therefore insignificant. This is easily understood due to the assumed bound $\widetilde{N}_1 \gtrsim 70$ GeV and the rough relations $m_{\widetilde{N}_2} \sim m_{\widetilde{C}_1} \sim 2m_{\widetilde{N}_1}$, which hold since μ is relatively large in our models.

The discovery process $e^+ e^- \rightarrow \widetilde{N}_1 \widetilde{N}_1$ with each $\widetilde{N}_1 \rightarrow \gamma\widetilde{G}$, leads to events with two energetic photons and large missing energy.[3] This signal has already been studied for LEP 2 in an earlier paper [30], but we will be able to extend these results. Also, Ref. [30] made no assumptions about model parameters; in taking into account the constraints inherent in the GMSB models we will be able to make some more concrete (and optimistic) statements. The most important point to be made in this regard is that in the GMSB neutralino NLSP models of the class described in Sec. II, the $\widetilde{N}_1 \widetilde{N}_1$ production cross section can be bounded from below for a given $m_{\widetilde{N}_1}$. This result is due to the facts that $\widetilde{N}_1$ is always gauginolike and $m_{\widetilde{e}_R}$ is bounded from above. The dominant t-channel exchange of $\widetilde{e}_R$ therefore always ensures a substantial cross section. To illustrate this, we show in Fig. 2 the minimum and maximum cross sections for $\widetilde{N}_1$ pair production obtained in these models, for $\sqrt{s} = 161$, 172, and 190 GeV. This graph was prepared by an exhaustive scan of the model parameter space, varying Λ, x, $\tan\beta$, and sgn(μ). The minimum cross sections are ob-

---

[3] We prefer not to use the words ''acoplanar photons'' to refer to this signal, since the acoplanarity seems not to be a particularly useful discriminant against background.
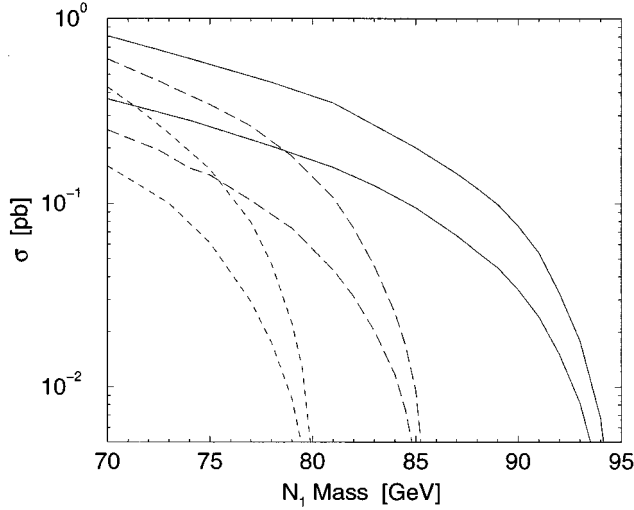
FIG. 2. The maximum and minimum cross sections for $e^+e^- \rightarrow \widetilde{N}_1\widetilde{N}_1$ at $\sqrt{s} = 161$ GeV (short dashed), 172 GeV (long dashed), and 190 GeV (solid), as a function of the mass of the lightest neutralino. These bounds hold in the neutralino NLSP models within the GMSB framework described in Sec. II.

tained for models with $n = 1$ and x not too large in which $m_{\widetilde{e}_R}/m_{\widetilde{N}_1}$ saturates its upper bound of about 1.6.

The energy of each $\widetilde{N}_1$ is equal to the beam energy $\sqrt{s}/2$, so that the photon energies in each event have a flat distribution, with

$$E_{\min} < E_{\gamma_1}, E_{\gamma_2} < E_{\max}, \tag{32}$$

where

$$E_{\max,\min} = \frac{1}{4} \left(\sqrt{s} \pm \sqrt{s - 4m_{\widetilde{N}_1}^2} \right). \tag{33}$$

Therefore one can always impose a cut on soft photons, depending on an assumed lower bound on the mass of the $\widetilde{N}_1$ being searched for. In this paper, we will (motivated by [30]) take $m_{\widetilde{N}_1} > 70$ GeV as a given, so that a cut

$$E_\gamma > \frac{1}{4} \left[\sqrt{s} - \sqrt{s - (140 \text{ GeV})^2} \right] \tag{34}$$

on soft photons can be applied without affecting the signal at all. The missing energy in each event is also bounded according to $2E_{\min} < \rlap{/}{E} < 2E_{\max}$.

The most important physics backgrounds for the $\gamma\gamma\rlap{/}{E}$ signal are due to $e^+e^- \rightarrow \gamma\gamma\nu_i\bar{\nu}_i$ from diagrams with s-channel Z exchange ($i = e, \mu, \tau$) and t-channel W exchange ($i = e$ only). These backgrounds were discussed in some detail in [30], where it was shown that they can be efficiently eliminated using a cut on the invariant missing mass $M_{\text{inv}}^2 \equiv (p_{e^+} + p_{e^-} - p_{\gamma 1} - p_{\gamma 2})^2$. The M_{inv} distribution of the signal tends to be broadly distributed and has most of its support for lower values than the background, which is strongly peaked at M_Z but with a significant tail due to the t-channel contributions. In Figs. 3 and 4 we show a comparison of the signal and background distributions for $\sqrt{s} = 172$
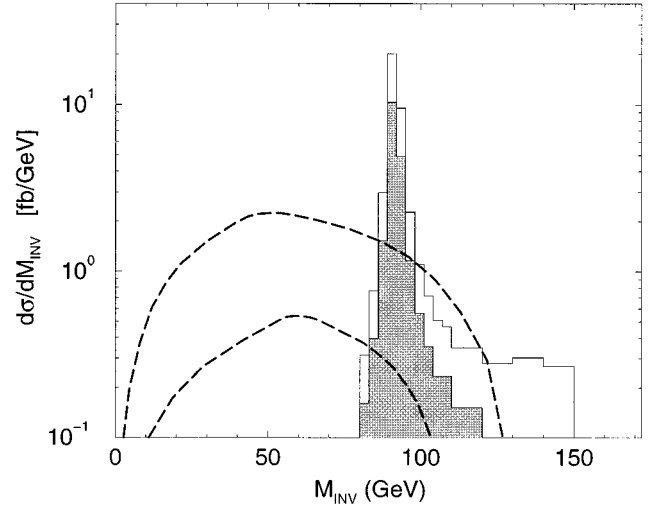

FIG. 3. Missing invariant mass distributions at $\sqrt{s} = 172$ GeV for $\gamma\gamma\rlap{/}{E}$ events which pass the cuts (35) and (36). The background from $e^+e^- \rightarrow \gamma\gamma\nu_i\bar{\nu}_i$ is shown as the open (shaded) histogram before (after) the photon energy cut $E_\gamma > 18$ GeV from Eq. (34). The upper (lower) dashed line is the signal distribution from $\widetilde{N}_1\widetilde{N}_1$ production for representative models with $m_{\widetilde{N}_1} = 75(82)$ GeV as described in the text.

and 190 GeV, respectively. In preparing these figures, we have applied detectability cuts [45]

$$|\cos\theta_\gamma| < 0.95, \tag{35}$$

$$(p_T)_\gamma > 0.0325\sqrt{s}, \tag{36}$$

for each photon. The background distributions before and after the cut on soft photons (34) were computed at tree-level using COMPHEP [46], and are shown as the open and shaded histograms. Also shown are the distributions for the signals
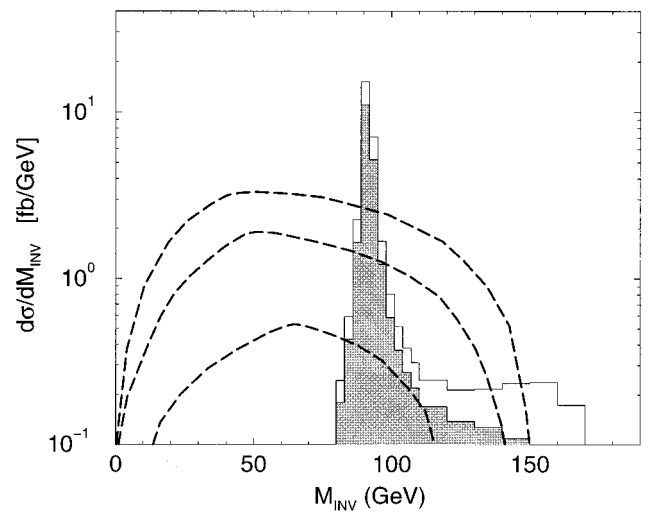

FIG. 4. Missing invariant mass distributions at $\sqrt{s} = 190$ GeV for $\gamma\gamma\rlap{/}{E}$ events which pass the cuts (35) and (36). The background from $e^+e^- \rightarrow \gamma\gamma\nu_i\bar{\nu}_i$ is shown as the open (shaded) histogram before (after) the photon energy cut $E_\gamma > 16$ GeV from Eq. (34). The dashed lines are the signal distributions from $\widetilde{N}_1\widetilde{N}_1$ production for representative models with $m_{\widetilde{N}_1} = 75, 82,$ and 90 GeV (from top to bottom) as described in the text.

TABLE I. The $\gamma\gamma\nu\bar{\nu}$ background to the $\gamma\gamma E\!\!\!/$ signal at LEP 172 and LEP 190, after the following cuts (described in the text): (1) $|\cos\theta_\gamma|<0.95$, (2) $(p_T)_\gamma>0.0325\sqrt{s}$, (3) $E_\gamma>\frac{1}{4}[\sqrt{s}-\sqrt{s-(140\,\text{GeV})^2}]$, (4) $M_{\text{inv}}<80\,\text{GeV}$. The missing invariant mass cut (4) clearly reduces the main background to a negligible level. The additional cut $M_{\text{inv}}>5\,\text{GeV}$ is needed to eliminate the background from $\gamma\gamma(\gamma)$, where (γ) is lost in either the detector or the beam pipe.

Cross section (fb) for $\sum_{i=e,\mu,\tau}\gamma\gamma\nu_i\bar{\nu}_i$ after			
$\sqrt{s}$ (GeV) cuts:	(1–2)	(1–3)	(1–4)
172	131	65.6	0.79
190	102	70.0	0.80

derived at tree-level from some sample models with $m_{\widetilde{N}_1}=75$, 82, and 90 GeV. These models were chosen with $n=1$, $\tan\beta=3$, $x=0.1$, and $\mu<0$. The shape (but not the magnitude) of the signal distributions is largely independent of these choices, for a fixed $\sqrt{s}$ and $m_{\widetilde{N}_1}$. This can be easily understood since the dominant kinematic features of these events are due to the isotropic decays $\widetilde{N}_1\to\gamma\widetilde{G}$. Besides the cuts Eqs. (34)–(36) we therefore propose to implement a cut on the missing invariant mass of

$$5\ \text{GeV}<M_{\text{inv}}<80\ \text{GeV}. \qquad (37)$$

The lower limit in Eq. (37) is designed to remove detector backgrounds such as $e^+e^-\to\gamma\gamma(\gamma)$ with the third photon unobserved. We expect that the effect of initial state radiation will be to reduce slightly the total magnitude of both the signal and the background, while not qualitatively affecting the shapes of M_{inv} distributions; in particular, after the cut Eq. (37), the background is still negligible.

At $\sqrt{s}=172$ GeV the total $\widetilde{N}_1\widetilde{N}_1$ production cross sections for the examples in Fig. 3 with $m_{\widetilde{N}_1}=75$ and 82 GeV are 195 and 41 fb, respectively, before any cuts. After the cuts Eqs. (34)–(37), the remaining background is less than 1 fb, while the signal for these models is 128 and 30 fb. With 10 pb^{-1} per detector, this amounts to an expectation of roughly 5 events and 1.2 events (summed over all four detectors).

At $\sqrt{s}=190$ GeV the total cross sections in the models of Fig. 4 are (350,180,41) fb for $m_{\widetilde{N}_1}=(75,82,90)$ GeV, respectively. After applying all of the cuts Eqs. (34)–(37), we find remaining signals of (193,106,25) fb. With 300 pb^{-1} per detector, this corresponds to about (58,32,7.5) events for each of the four detectors. The remaining background after these cuts is less than 1 fb.

As shown by these examples, the efficiency for detecting signal events after cuts is quite high, while the physics background is essentially completely eliminated. The effects of the cuts on the backgrounds are shown in Table I. In Fig. 5, we show the efficiency (defined as the fraction of signal events which pass all of our cuts divided by the total number of signal events) as a function of $m_{\widetilde{N}_1}$ for various beam energies $\sqrt{s}=161$, 172, 185, 190, 195, and 200 GeV. The efficiency decreases slightly with increasing beam energy, but always exceeds 50%. Also, we note that the efficiency increases slightly closer to threshold; this is because nearer
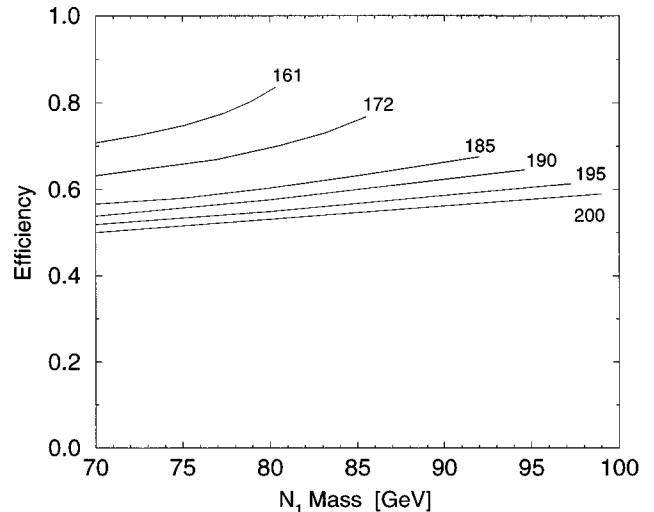

FIG. 5. The fraction of $\gamma\gamma E\!\!\!/$ events from neutralino pair production which pass the detector cuts (35), (36), and missing invariant mass cut (37). The lines from top to bottom are for $\sqrt{s}=161$, 172, 185, 190, 195, and 200 GeV. Here we have chosen a representative class of models as described in the text, but for fixed $m_{\widetilde{N}_1}$ and $\sqrt{s}$ the efficiency is quite insensitive to variations in model parameters.

threshold the M_{inv} distribution for the signal becomes somewhat more sharply peaked with a smaller overlap with the cut region $M_{\text{inv}}>80$ GeV. The plotted efficiencies were found for a specific class of models with $n=1$, $\tan=3$, $x=0.1$, $\mu<0$ and varying Λ, but these results are very nearly model independent for a fixed $m_{\widetilde{N}_1}$, since the efficiencies depend mostly on the kinematics of the isotropic $\widetilde{N}_1$ decays. Therefore one may estimate the usable cross section (after all cuts) for future LEP 2 runs by simply multiplying the total cross section by 0.5. While the LEP runs at $\sqrt{s}=161,172$ were limited by only having ~10 pb^{-1} collected per experiment, the reach at $\sqrt{s}=172$ GeV extends even beyond $m_{\widetilde{N}_1}=77$ GeV in some parts of the GMSB model parameter space. However, considering the minimum cross section obtained in some models (see Fig. 2), the exclusion capability for these runs is about $m_{\widetilde{N}_1}>72$ GeV, using a criterion of five total events (summed over all four detectors) after all cuts. This limit is quite comparable to what should be attainable with the present Tevatron data (and provides *a posteriori* justification for our assumption $m_{\widetilde{N}_1}>70$ GeV). With 300 pb^{-1} and a discovery requirement of five events after cuts, the discovery reach should extend up to about $m_{\widetilde{N}_1}=\sqrt{s}/2-4$ GeV in future runs, based on an efficiency of 50%. If a discovery is made, the events with the largest photon energies can be used to find $m_{\widetilde{N}_1}$ using Eqs. (32) and (33). (The lower endpoint of the energy range will be contaminated with $\gamma\gamma\nu\bar{\nu}$ background events.)

We note that observation of a few $\gamma\gamma E\!\!\!/$ events with $M_{\text{inv}}>80$ GeV could not be interpreted as unambiguous evidence for $\widetilde{N}_1\widetilde{N}_1$ production, since the background is comparable to or larger than the signal, especially if our cut on soft photons (34) is not applied. Conversely any events with $M_{\text{inv}}<80$ GeV would be of great interest for the GMSB sce-

nario, since the physics backgrounds for such events are quite negligible.[4]

When kinematically allowed, slepton pair production can add to the main $\widetilde{N}_1\widetilde{N}_1$ discovery signal. Each of the production cross sections for $\widetilde{e}_R\widetilde{e}_R$, $\widetilde{\mu}_R\widetilde{\mu}_R$, and $\widetilde{\tau}_1\widetilde{\tau}_1$ can even exceed 0.1 pb at $\sqrt{s}=190$ GeV, adding events $l^+l^-\gamma\gamma\not{E}$ to the $\gamma\gamma\not{E}$ signal we have just discussed. The leptons in these events should be softer than the photons, because the slepton production cross section cannot be significant unless $m_{\widetilde{l}}-m_{\widetilde{N}_1}$ is small. For some models with large $\tan\beta$, only $\widetilde{\tau}_1\widetilde{\tau}_1$ pair production with signal $\tau^+\tau^-\gamma\gamma\not{E}$ can occur in addition to $\gamma\gamma\not{E}$. While the individual slepton pair production cross sections never exceed half of the $\widetilde{N}_1\widetilde{N}_1$ production cross section, the $l^+l^-\gamma\gamma\not{E}$ signal(s) should not have any significant backgrounds (especially considering that the photons are always energetic). Therefore it should be kept in mind that slepton pair production can be an important component of the discovery signal even in the neutralino NLSP scenario. In the minimal model with $n=1$, this can only occur if x is significantly greater than 0, so that observation of both $\gamma\gamma\not{E}$ and $l^+l^-\gamma\gamma\not{E}$ at LEP 2 would exclude models with $n=1$ and small relative mass splittings for the messenger fields.

B. The slepton co-NLSP scenario

In this subsection we consider the case that $\widetilde{\tau}_1$, $\widetilde{e}_R$, and $\widetilde{\mu}_R$ are lighter than all of the other superpartners, and are nearly degenerate in mass. As long as the conditions Eq. (11) are satisfied, then $\widetilde{\tau}_1$, $\widetilde{e}_R$, $\widetilde{\mu}_R$ act effectively as co-NLSP's each decaying directly to the corresponding lepton plus gravitino. This situation can arise if $n=2$, 3, or 4, and $\tan\beta\lesssim8$. For larger values of $\tan\beta$, the tau Yukawa coupling causes mixing between the left- and right-handed staus which is always sufficient to render $m_{\widetilde{\tau}_1}$ lower than $m_{\widetilde{\mu}_R}$ by more than the τ mass. Restricting our attention to models with slepton NLSP masses between 50 and 100 GeV, we find that the allowed ranges for the parameter Λ are

$$n=2; \quad 15 \text{ Tev}<\Lambda<42 \text{ TeV, or} \tag{38}$$

$$n=3; \quad 11 \text{ Tev}<\Lambda<35 \text{ TeV, or} \tag{39}$$

$$n=4; \quad 10 \text{ Tev}<\Lambda<28 \text{ TeV,} \tag{40}$$

in order for Eq. (11) to be satisfied. As mentioned in the Introduction, however, there are some models for which $m_{\widetilde{l}_R}-m_{\widetilde{\tau}_1}-m_\tau-m_l$ can be up to a few GeV but $\widetilde{l}_R\rightarrow l\widetilde{G}$ can still dominate if $\sqrt{F}$ is not too large and $\widetilde{l}_R\rightarrow l\widetilde{N}_1$ is not kinematically open. Those models will also act as slepton co-NLSP models. In any case, using Eqs. (5) and (25), we find that the minimum possible decay length at LEP 2 in the slepton co-NLSP scenario is about 10 μm for $n=2$, and

---

[4]We also note that in the Higgsino LSP interpretation [28,47] of the CDF event [39], one could conceivably have $\gamma\gamma\not{E}$ events from $\widetilde{N}_2\widetilde{N}_2$ production with the one-loop decay $\widetilde{N}_2\rightarrow\gamma\widetilde{N}_1$, but these would yield softer photons, and as with the background would tend to have larger M_{inv} than a GMSB signal.
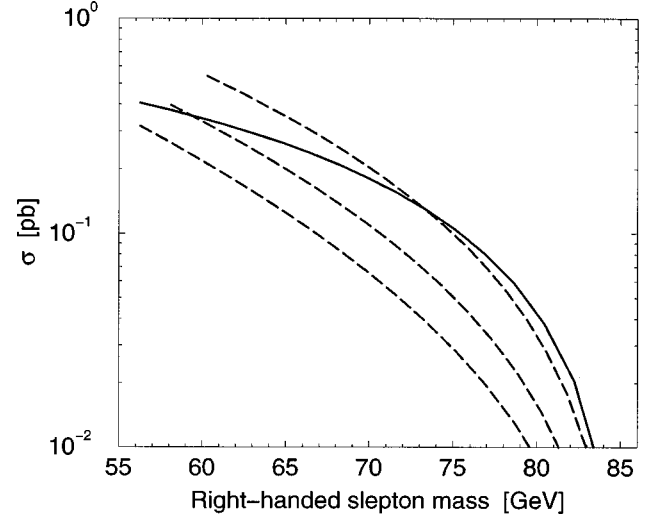

FIG. 6. Slepton pair production cross sections as a function of slepton mass, for e^+e^- collisions at $\sqrt{s}=172$ GeV. The solid curve is the (model-independent) production cross section for $\widetilde{\mu}_R\widetilde{\mu}_R$. The three dashed lines are the $\widetilde{e}_R\widetilde{e}_R$ production cross sections for a family of models with varying Λ and fixed $x=0.1$, $\mu<0$, $\tan\beta=1.5$, and, from top to bottom, $n=2,3,4$. (The model dependence is due to the t-channel exchange of neutralinos.) The $\widetilde{\tau}_1\widetilde{\tau}_1$ production cross section in slepton co-NLSP models is always nearly equal to that of $\widetilde{\mu}_R\widetilde{\mu}_R$.

somewhat smaller for $n=3,4$. Of course, values of $x\lambda$ smaller than 1 will increase the decay length proportionally to $1/(x\lambda)^2$, and $F_S<F$ would have the same effect. This means that the $\widetilde{l}\rightarrow l\widetilde{G}$ decay lengths can easily exceed minimum detector resolutions, providing a background-independent signal [26,34] if the tracks of stable sleptons and/or their macroscopic decay lengths are observed by the LEP 2 detectors. This would be spectacular confirmation of the GMSB scenario.

The cross section for $\widetilde{\mu}_R\widetilde{\mu}_R$ production at LEP 2 (as a function of $m_{\widetilde{\mu}_R}$) is model independent, since this process is mediated only by s-channel exchange of γ,Z. The $\widetilde{e}_R\widetilde{e}_R$ pair production cross section has a contribution from t-channel neutralino exchange, but there is significant destructive interference with the s-channel γ,Z exchange graphs, especially near threshold. This means that $\sigma(\widetilde{e}_R\widetilde{e}_R)$ is often much lower than $\sigma(\widetilde{\mu}_R\widetilde{\mu}_R)$ in slepton co-NLSP GMSB models. This is an important qualitative difference from the situation in neutralino LSP models as studied in [43,44], where exchange of a lighter neutralino in the t channel typically ensures that $\sigma(\widetilde{e}_R\widetilde{e}_R)>\sigma(\widetilde{\mu}_R\widetilde{\mu}_R)$. The destructive interference effect in slepton co-NLSP models is greater for larger values of n, corresponding to heavier $\widetilde{N}_1$. We find that in our slepton co-NLSP model parameter space $\sigma(\widetilde{e}_R\widetilde{e}_R)<\sigma(\widetilde{\mu}_R\widetilde{\mu}_R)$ always holds for $m_{\widetilde{l}_R}$ more than about (10,16,20) GeV below the kinematic threshold of $\sqrt{s}/2$, for models with $n=(2,3,4)$.

These features are illustrated in Figs. 6 and 7, which show production cross sections in e^+e^- collisions at $\sqrt{s}=172$ and 190 GeV for $\widetilde{e}_R\widetilde{e}_R$ and $\widetilde{\mu}_R\widetilde{\mu}_R$. The results shown for $\widetilde{e}_R\widetilde{e}_R$ are for a typical family of GMSB models with $x=0.1$, $\tan\beta=1.5$, $\mu<0$ and Λ varying, as a function of $m_{\widetilde{\mu}_R}\approx m_{\widetilde{e}_R}$. The three dashed lines in Figs. 6 and 7 are the
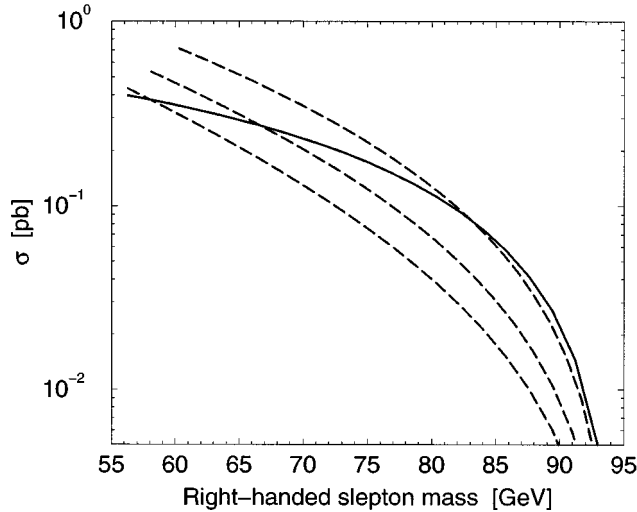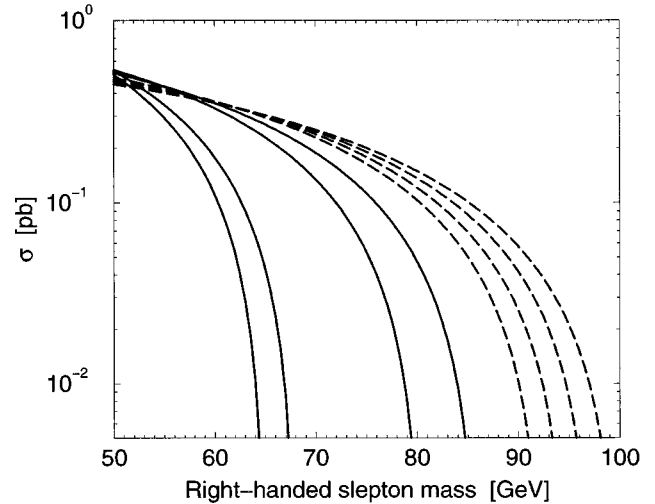
FIG. 7. As in Fig. 6, but with $\sqrt{s} = 190$ GeV.

FIG. 8. Smuon pair production cross sections as a function of $m_{\widetilde{\mu}_R}$, for e^+e^- collisions at (from left to right) $\sqrt{s} = 130$, 136, 161, 172 (solid lines) and 185, 190, 195, and 200 GeV (dashed lines).

$\widetilde{e}_R\widetilde{e}_R$ cross sections in this class of models for $n = 2,3,4$ from top to bottom. (These models have lower bounds on $m_{\widetilde{l}_R}$ as indicated; these follow indirectly from a lower bound on the mass of the lightest Higgs boson, which we take to be $m_h < \sin^2(\beta - \alpha)64$ GeV [48].) For a given n, the $\widetilde{e}_R\widetilde{e}_R$ production cross sections in other models can be up to a factor of 2 smaller, but not much larger, than shown in Figs. 6 and 7. The production cross section for $\widetilde{\tau}_1\widetilde{\tau}_1$ is always nearly equal to that for $\widetilde{\mu}_R\widetilde{\mu}_R$, owing to the small mixing required by low $\tan\beta$ and near degeneracy of $\widetilde{\mu}_R$ and $\widetilde{\tau}_1$. For a given model, one finds that $\sigma(\widetilde{\tau}_1\widetilde{\tau}_1)$ exceeds $\sigma(\widetilde{\mu}_R\widetilde{\mu}_R)$ by a few per cent.

With the 10 pb^{-1} collected at $\sqrt{s} = 172$ GeV it is apparent from Fig. 6 that, modulo detector-dependent considerations regarding the rate of energy loss by ionization and tracking chamber capabilities, one should be able to put a useful exclusion on long-lived sleptons. Indeed, the DELPHI collaboration has recently analyzed data from runs with $\sqrt{s} \leqslant 161$, 172 GeV, and found that long-lived right-handed smuons and staus with mass less than 65 GeV are excluded at the 95% confidence level [49]. A somewhat more restrictive lower bound could presumably be obtained by combining the results of all four detectors. Likewise, searches for sleptons with decay lengths exceeding several centimeters could probably establish similar limits. Comparing with Fig. 7, we see that in future runs with 300 pb^{-1} or more, it should be possible to exclude or discover long-lived sleptons with masses up to a few GeV of the kinematic limit. (Comparable constraints on long-lived sleptons from the present Tevatron data will probably be difficult to obtain [50].)

In the remainder of this subsection, we concentrate on the more difficult situation that the finite decay lengths for the sleptons are too short to measure. The signals for slepton pair production are then $e^+e^-\not{E}$, $\mu^+\mu^-\not{E}$, or $\tau^+\tau^-\not{E}$ for $\widetilde{e}_R\widetilde{e}_R$, $\widetilde{\mu}_R\widetilde{\mu}_R$, $\widetilde{\tau}_1\widetilde{\tau}_1$, respectively [26]. As illustrated by the examples of Figs. 6 and 7, the worst-case situation for a given $m_{\widetilde{l}_R}$ will have $\sigma(\widetilde{e}_R\widetilde{e}_R) \ll \sigma(\widetilde{\mu}_R\widetilde{\mu}_R)$, so we concentrate on $\widetilde{\mu}_R\widetilde{\mu}_R$ as the discovery process. (In general, $\widetilde{e}_R\widetilde{e}_R$ can be the dominant discovery process in slepton co-NLSP models only when both cross sections are large and discovery is relatively easy anyway.) In Fig. 8, we show the model-independent production cross section for $\widetilde{\mu}_R\widetilde{\mu}_R$ as a function of $m_{\widetilde{\mu}_R}$, for

various beam energies. The past LEP runs at $\sqrt{s} = 130$–136, 161, and 172 GeV collected about 5.7, 10, and 10 pb^{-1} per detector, respectively. Slepton masses less than about 55 GeV would have resulted in several $l^+l^-\not{E}$ events for each detector at LEP 130–136, with a detection efficiency probably well in excess of 50%, since the decays $\widetilde{l} \rightarrow l\widetilde{G}$ will always result in energetic leptons. (See for example the analogous situation analyzed in [51] in the case of sleptons decaying to a lepton and light neutralino.) For the LEP 161 and LEP 172 runs, several events per detector could be expected for slepton masses up to perhaps 70 GeV, but with a background from W^+W^- production with leptonic W decays, as discussed below. A precise determination of slepton mass exclusions from present data in the slepton co-NLSP case would involve detector-specific issues and will not be attempted here.

Future runs with higher beam energy and much more data should be able to decisively probe a significant range of slepton masses. The lepton energies in each event have a flat distribution (before any cuts) with endpoints given by

$$E_{\min} < E_{l^+}, \ E_{l^-} < E_{\max}, \tag{41}$$

where

$$E_{\max,\min} = \frac{1}{4}(\sqrt{s} \pm \sqrt{s - 4m_{\widetilde{l}}^2}). \tag{42}$$

Therefore the leptons from the signal events are quite energetic (especially in the critical case that $m_{\widetilde{l}}$ is near the kinematic threshold so that the production cross section is low), allowing one to choose a rather strong cut on the minimum lepton energy. To reduce an important component of the background as discussed below, it is necessary to impose such a lower bound on lepton energy (in contrast to the situation for slepton signals with a neutralino LSP [43,44], where it is instead useful to impose an upper bound cut on lepton energies). We will somewhat arbitrarily take this to be

$$E_l > 20 \text{ GeV}, \tag{43}$$

TABLE II. The dominant backgrounds to dilepton signals at $\sqrt{s}=190$ GeV after the following cuts (described in the text): (1) $|\eta_l|<2.5$, (2) $\not{p}_T>0.05\sqrt{s}$, (3) $\cos\phi(l^+l^-)>-0.9$, (4) $|M_{\mathrm{inv}}-M_Z|>10$ GeV, (5) $E_l>20$ GeV, (6) $\pm\cos\theta_{l\pm}>0$. Other channels [e.g., $\nu\bar{\nu}Z(\rightarrow l^+l^-)$, $\mu^\pm\nu_\mu W^\mp(\rightarrow\mu^\mp\nu_\mu)$, contributions to $\mu^+\mu^-Z$ from processes other than γ^*Z and ZZ production, multiperipheral diagrams, etc.] produce additional backgrounds at the level of 1 fb or less, before cuts. Cuts (1–2) are needed to reduce backgrounds from $e^+e^-(\gamma)$, $e^+e^-(l^+l^-)$, where (x) means x is lost in the beam pipe, as well as to ensure final state detection. Cut (3) is necessary to eliminate the background from $\tau^+(\rightarrow l^+\nu\nu)\tau^-(\rightarrow l^-\nu\nu)$ and is also quite effective in reducing (a), (b), (d) and (e) [by about 24, 23, 18, and 15 % of the corresponding respective amounts after cuts (1–2)]. Note that the processes (d) and (e) are backgrounds only for the $e^+e^-\not{E}$ signal.

Background ($l=e$ or μ)	cuts:	Cross section (fb) at LEP 190 after			
		(1–3)	(1–4)	(1–5)	(1–6)
(a) $W^+W^-\rightarrow l^+l^-\nu_l\bar{\nu}_l$		163	141	140	22.3
(b) $W^+W^-\rightarrow l^\pm\tau^\mp(\rightarrow l^\mp\nu_\tau\nu_l)\nu_l\nu_\tau$		57.2	42.5	17.7	3.03
(c) $\sum_{i=e,\mu,\tau}\gamma^*(\rightarrow l^+l^-)Z(\rightarrow\nu_i\bar{\nu}_i)$		31.2	2.97	0.83	0.40
(d) $\sum_{i=e,\mu,\tau}e^+e^-Z(\rightarrow\nu_i\bar{\nu}_i)$ (other than ZZ, γ^*Z contribs.)		14.8	0.93	0.56	0.13
(e) $\Sigma_\pm\,e^\pm\nu_e W^\mp(\rightarrow e^\mp\nu_e)$		13.9	11.4	7.69	1.96
(f) $\sum_{i=e,\mu,\tau}Z(\rightarrow l^+l^-)Z(\rightarrow\nu_i\bar{\nu}_i)$		4.92	0.27	0.27	0.13

which does not impact the signal at all for $m_{\tilde{l}}>77.5$ GeV for $\sqrt{s}=190$ GeV, but this can and should be adjusted depending on the signal and on the collider parameters. In the following discussion we also impose a detectability cut

$$|\eta_l|<2.5 \qquad (44)$$

on the pseudorapidity of each lepton.

The fraction of $e^+e^-\not{E}$, $\mu^+\mu^-\not{E}$, and $\tau^+\tau^-\not{E}$ signal events which pass these cuts is always quite high. Unfortunately, there are significant backgrounds to these signals which must be considered. First, one has $e^+e^-\rightarrow\tau^+\tau^-$ with leptonic τ decays which gives a background to $l^+l^-\not{E}$ with $l=e,\mu$. The resulting leptons are always nearly back-to-back, so that an acoplanarity cut

$$\cos\phi(l^+l^-)>-0.9 \qquad (45)$$

can essentially eliminate this background, while leaving the signal largely intact. (The angle ϕ is defined between the two leptons in the plane transverse to the beam axis.) Backgrounds from $l^+l^-\gamma$ and $l^+l^-e^+e^-$ production with the photon or e^+e^- lost down the beampipe can be efficiently eliminated with a cut on the total missing transverse momentum [43]

$$\not{p}_T>0.05\sqrt{s}. \qquad (46)$$

Significant backgrounds also arise from $e^+e^-\rightarrow Z(\rightarrow\nu\bar{\nu})\gamma^*(\rightarrow l^+l^-)$ and $e^+e^-\rightarrow Z(\rightarrow\nu\bar{\nu})Z(\rightarrow l^+l^-)$. To eliminate them we impose a cut

$$|M_{\mathrm{inv}}-M_Z|>10 \text{ GeV} \qquad (47)$$

on the missing invariant mass $M_{\mathrm{inv}}\equiv(p_{e_i^+}+p_{e_i^-}-p_{l_f^+}$ $-p_{l_f^-})^2$ in each event. Other minor backgrounds are present from higher order processes such as $e^+e^-\rightarrow e\nu W(\rightarrow e\nu)$. Their sizes before and after our cuts are given in Table II, where we show that they are reduced to a negligible level. It should be noted that these cuts will also reduce any potentially dangerous interferences of these backgrounds with the main background we are about to discuss.

When $\sqrt{s}>2M_W$, the largest physics background is due to W-pair production followed by leptonic W decays:

$$e^+e^-\rightarrow W^+W^-\rightarrow l^+l^-\nu\bar{\nu}. \qquad (48)$$

At $\sqrt{s}=190$ fb, this background amounts to 238 fb for each lepton flavor, before cuts. This is reduced to 140 fb after applying the cuts Eqs. (43)–(47). The kinematics of the background (48) are similar to those of the slepton pair-production signal, especially if $m_{\tilde{l}}$ is close to m_W, and in particular the cut (43) has only a very small effect. The situation is rather similar to the case of slepton pair production at LEP in the neutralino LSP scenario as studied in [43,44], but with $\tilde{l}\rightarrow l\tilde{G}$ taking the place of $\tilde{l}\rightarrow l\tilde{N}_1$. Note that in the present situation, the near masslessness of the gravitino makes the decay $\tilde{l}\rightarrow l\tilde{G}$ even more kinematically similar to the standard model decay $W\rightarrow l\nu$. In particular, the signal cannot be enhanced significantly by imposing an upper bound on the lepton energies, as it could be in the situation investigated in [43,44]. However, we can still use the fact that the positively (negatively) charged leptons from W^+W^- production are produced preferentially in the same direction as the positron (electron) beam. This polar angle

asymmetry also unfortunately holds true for the $e^+e^-\not{E}$ signal from $\widetilde{e}_R\widetilde{e}_R$ production, although not as strongly as for the background. The $\mu^+\mu^-\not{E}$ and $\tau^+\tau^-\not{E}$ signals are fortunately symmetric with respect to $\theta\rightarrow\pi-\theta$ because $e^+e^-\rightarrow\widetilde{\mu}_R\widetilde{\mu}_R$ and $e^+e^-\rightarrow\widetilde{\tau}_1\widetilde{\tau}_1$ production have only s-channel contributions. Therefore the signal/background ratio for $\widetilde{\mu}_R\widetilde{\mu}_R$ and $\widetilde{\tau}_1\widetilde{\tau}_1$ (and to a lesser extent $\widetilde{e}_R\widetilde{e}_R$) can be significantly enhanced by imposing a cut

$$\pm\cos\,\theta_{l\pm}>0 \qquad (49)$$

on the more energetic lepton in each event, as in [43,44]. (We always use the definition of θ as the angle between the e^- beam momentum and the outgoing lepton momentum.)

We must also consider a background contribution for $e^+e^-\not{E}$ and $\mu^+\mu^-\not{E}$ (but not for $\tau^+\tau^-\not{E}$) from

$$e^+e^-\rightarrow W^+W^-\rightarrow l^\pm\tau^\mp\nu\overline{\nu}\rightarrow l^+l^-\nu\overline{\nu}\nu\overline{\nu}. \qquad (50)$$

Since $\tau\rightarrow l\nu\overline{\nu}$ has a branching fraction of about 0.18 for each of $l=e,\mu$, a rough estimate is that the additional $l^+l^-\not{E}$ backgrounds are each about 0.36 times the direct $W^+W^-\rightarrow l^+l^-\nu\overline{\nu}$ background. However, this is an overestimate, since the resulting leptons tend to be softer so that a large fraction of these events are eliminated by the minimum energy cut (43), which was included for this reason. Before (after) the cuts Eqs. (43)–(47) this background contributes 84 (18) fb. It should be noted that if some efficient tau tagging is possible, then some part of this background could be eliminated. However, this is a highly detector-dependent matter and we choose to simply consider the whole background. There is also a background from $e^+e^-\rightarrow W^+W^-\rightarrow\tau^+\tau^-\nu\overline{\nu}\rightarrow l^+l^-\nu\overline{\nu}\nu\overline{\nu}$, but this is suppressed by the factor $B(\tau\rightarrow l\nu\overline{\nu})^2\approx0.03$ and is greatly diminished further by the cut (43), and so can be safely neglected. In Table II we summarize the dominant $l^+l^-\not{E}$ backgrounds showing the effects of the cuts described above.

To evaluate the background from Eq. (50) we used our own Monte Carlo simulating the tau decay following each of the parent $WW\rightarrow\mu\tau\nu\nu$ events generated using COMPHEP and the BASES-SPRING package [52]. In doing this, we also took into account spin correlations and tau-decay anisotropies in the tau rest frame. We checked that neglecting the latter effects would have resulted in an 18% underestimate of this background after cuts (1–5) in Table II and in an only slightly flatter distribution in $\pm\cos\theta_{l\pm}$ so that the underestimate is diminished to 17% after cuts (1–6). The effect of taking into account spin correlations is not dramatic in this case because the pattern of distributions is dominated by a large boost of the tau in the lab frame.

These considerations are illustrated in Fig. 9, which shows the distribution of $\pm\cos\theta_{l\pm}$ for the $\widetilde{\mu}_R\widetilde{\mu}_R$ and $\widetilde{e}_R\widetilde{e}_R$ signals in a model with $m_{\widetilde{l}_R}=80$ GeV. (The other model parameters, which do not affect the distribution from smuons, were chosen to be $n=3$, $\Lambda=24$ TeV, $\tan\beta=1.5$, $x=0.1$, with $\mu=-460$ GeV.) Also shown as the heavier solid line histogram is the distribution for background events from both Eqs. (48) and (50). The $\mu^+\mu^-\not{E}$ component of the signal is much more promising than $e^+e^-\not{E}$, both because the total cross section is larger and because the polar angular distribution is less similar to the background. This is a quite
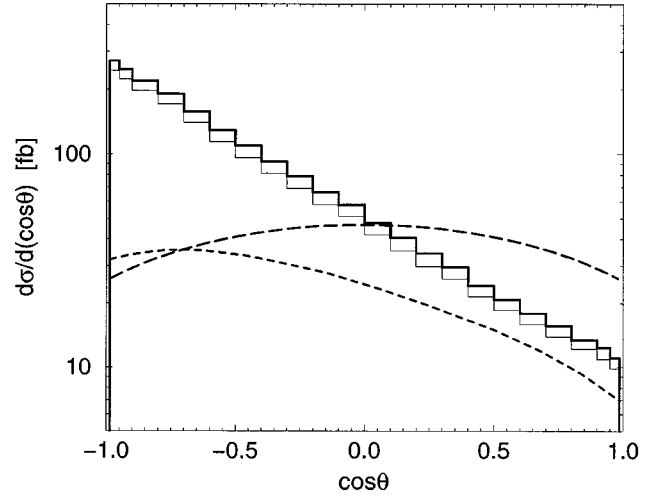

FIG. 9. The differential cross section $d\sigma/d(\pm\cos\theta_{l\pm})$ for the more energetic lepton in each event at $\sqrt{s}=190$ GeV, after the cuts (43)–(47). The long-dashed (short-dashed) line is the signal from $e^+e^-\rightarrow\widetilde{l}^+\widetilde{l}^-\rightarrow l^+l^-\not{E}$ for muons (electrons), respectively. For this figure we have chosen a model with $m_{\widetilde{l}_R}=80$ GeV as described in the text. The lighter solid line histogram shows the background contribution from $e^+e^-\rightarrow W^+W^-\rightarrow l^+l^-\nu\overline{\nu}$ (not summed over lepton flavors), while the heavier solid line histogram includes also the background from $e^+e^-\rightarrow W^+W^-\rightarrow l^\pm\tau^\mp\nu\overline{\nu}\rightarrow l^+l^-\nu\overline{\nu}\nu\overline{\nu}$, where $l=e$ or μ.

general feature. In the case of the $\tau^+\tau^-\not{E}$ signal, there is no background from Eq. (50), so we also show in Fig. 9 the distribution from Eq. (48) only, as the lighter solid line histogram. (The $\tau^+\tau^-\not{E}$ signal is, however, subject to a significant and quite detector-dependent loss from τ identification efficiencies.)

As these examples illustrate, we may concentrate on $\widetilde{\mu}_R\widetilde{\mu}_R$ production as the likely discovery process, at least in the pessimistic but common situation that $\sigma(\widetilde{e}_R\widetilde{e}_R)\lesssim\sigma(\widetilde{\mu}_R\widetilde{\mu}_R)$. In Fig. 10 we compare the distributions for the
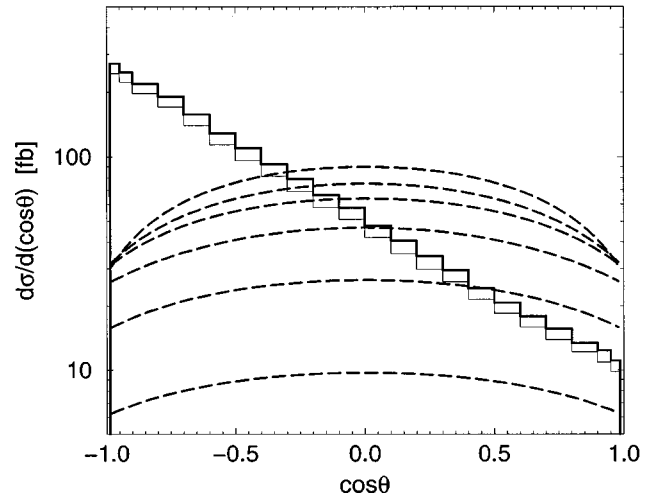

FIG. 10. The differential cross section $d\sigma/d(\pm\cos\theta_{l\pm})$ for the more energetic muon in each event at $\sqrt{s}=190$ GeV, after the cuts (43)–(47). The dashed lines are the signal from $e^+e^-\rightarrow\widetilde{\mu}_R\widetilde{\mu}_R\rightarrow\mu^+\mu^-\not{E}$ for, from the top down, $m_{\widetilde{\mu}_R}=60,70,75,80,85,90$ GeV. The background distributions are shown as described in Fig. 9.

polar angle of the more energetic muon from background and signal events, for various $\widetilde{\mu}_R$ masses. The W^+W^- background should contain $e^+e^-\not{E}$, $\mu^+\mu^-\not{E}$, $e^+\mu^-\not{E}$, and $e^-\mu^+\not{E}$ events in equal amounts. Meanwhile the signal yields more $\mu^+\mu^-\not{E}$ than $e^+e^-\not{E}$ events after the cut Eq. (49), and no $e\mu\not{E}$ events [except from $\widetilde{\tau}_1\widetilde{\tau}_1$ production with both taus decaying leptonically; this signal is again strongly diminished by the square of the leptonic branching fraction of the tau and by the energy cut Eq. (43)]. The cross sections at $\sqrt{s}=190$ GeV for signal $\mu^+\mu^-\not{E}$ events before cuts are $(360,238,178,121,69,25)$ fb for $m_{\widetilde{\mu}_R}=(60,70,75,80,85,90)$ GeV, respectively. The corresponding amounts which pass all of the cuts including Eq. (49) are $(70,60,52,39,23,8.5)$ fb, respectively. This amounts to an expectation of $(21,18, 16,12,7,2.5)$ signal $\mu^+\mu^-\not{E}$ events per detector with 300 pb^{-1}. For comparison, the total $\mu^+\mu^-\not{E}$ background from Eqs. (48), (50), and other sources which survives all of the cuts including Eq. (49) is 26 fb (see Table II), or 7.8 events in 300 pb^{-1}. Combining the results of all four detector should therefore give a 5σ discovery signal for $m_{\widetilde{l}_R}$ up to 85 GeV. However, we conclude from Fig. 10 that an unambiguous discovery may not be possible for models with $m_{\widetilde{\mu}_R}\gtrsim 85$ GeV, even with 300 pb^{-1} per experiment at $\sqrt{s}=190$ GeV, because of the low rates and significant WW background.[5]

In the delicate region where one is searching for smuons with $m_{\widetilde{\mu}_R}>80$ GeV, it will help to increase the minimum muon energy cut Eq. (43) and to impose an upper bound cut on muon energies, in view of Eq. (42), since this will reduce the W^+W^- backgrounds somewhat. It may also be useful to adjust the polar angle cut (49). The optimal cuts clearly depend in a nontrivial way on the beam energy, on the amount of integrated luminosity available, and on the masses of the sleptons being searched for, because of the low signal rates. If a discovery is made, the events with the highest muon energy Eq. (43) should provide the best estimate of the smuon mass using Eq. (42), if $m_{\widetilde{\mu}_R}<80$ GeV. For $m_{\widetilde{\mu}_R}\gtrsim 80$ GeV, such a determination will be more difficult because of the lower rates and because the range of muon energies from the signal events is entirely covered by the background.

It is important to note that when kinematically allowed, $\widetilde{N}_1\widetilde{N}_1$ will likely provide the clearest discovery signal. Despite $m_{\widetilde{N}_1}>m_{\widetilde{\tau}_1},m_{\widetilde{e}_R},m_{\widetilde{\mu}_R}$ in these models, we find that $\sigma(\widetilde{N}_1\widetilde{N}_1)$ can be as much as 3 times larger than $\sigma(\widetilde{\mu}_R\widetilde{\mu}_R)$ in the slepton co-NLSP scenario. Each $\widetilde{N}_1$ can decay as $\widetilde{N}_1\to\widetilde{l}_Rl\to l^+l^-\widetilde{G}$ or $\widetilde{N}_1\to\widetilde{\tau}_1\tau\to\tau^+\tau^-\widetilde{G}$. The first lepton emitted in the decay chain will often be very soft (if $m_{\widetilde{N}_1}-m_{\widetilde{l}_R}$ or $m_{\widetilde{N}_1}-m_{\tau_1}-m_\tau$ is small), but this does not degrade the signal. The reason is that because of the Majorana nature of $\widetilde{N}_1$, the charges and flavors of the two most energetic

leptons in the event (which carry most of the visible energy) are uncorrelated with each other. Therefore one has the rather unique signature of $l^+l'^+(l^-l'^-)\not{E}$ and $l^-l'^-(l^+l'^+)\not{E}$ and $l^+l'^-(l^-l'^+)\not{E}$ events in the ratio 1:1:2, with the leptons in parentheses being much softer, perhaps even too soft to detect. Here l and l' can each be e, μ, or τ, independently. Even if both soft leptons are not detected, the presence of two energetic same-charge leptons with large missing energy should be an unmistakable discovery signal for the first two of these signatures. (The analogue of this signal in the special case of a stau NLSP scenario was recently discussed in [37].) The $\widetilde{N}_1\widetilde{N}_1$ production cross section in slepton co-NLSP models is still bounded from below as in Fig. 2 (as a function of $m_{\widetilde{N}_1}$), but can also be much larger. We therefore find that the $\widetilde{N}_1\widetilde{N}_1$ channel will generally provide the largest discovery signal in slepton co-NLSP models if $m_{\widetilde{N}_1}$ is more than about 5 GeV below threshold. This is particularly likely to happen in models with $n=2$, for which $\widetilde{N}_1$ tends to be not much heavier than the sleptons. It is also especially probable when $\sigma(\widetilde{e}_R\widetilde{e}_R)$ and $\sigma(\widetilde{\mu}_R\widetilde{\mu}_R)$ are also both large, so that identifying an excess of $e^+e^-\not{E}$ and $\mu^+\mu^-\not{E}$ events above the WW backgrounds will also not be difficult. In that case the slepton pair production and $\widetilde{N}_1\widetilde{N}_1$ pair production signals should provide strong confirmation of each other.

C. The stau NLSP scenario

In this section we consider the case that the lightest stau is the NLSP and all supersymmetric decay chains terminate in $\widetilde{\tau}_1\to\tau\widetilde{G}$. Restricting our attention to $\widetilde{\tau}_1$ masses between 50 and 100 GeV, we find that the condition Eq. (10) can be satisfied in the GMSB model parameter space of Sec. II only if

$$n=1;\quad 35\ \text{TeV}<\Lambda<120\ \text{TeV};\quad \tan\beta>18,\ \text{or} \tag{51}$$

$$n=2;\quad 18\ \text{TeV}<\Lambda<80\ \text{TeV};\quad \tan\beta>6,\ \text{or} \tag{52}$$

$$n=3;\quad 12\ \text{TeV}<\Lambda<70\ \text{TeV};\quad \tan\beta>5,\ \text{or} \tag{53}$$

$$n=4;\quad 10\ \text{TeV}<\Lambda<60\ \text{TeV};\quad \tan\beta>4. \tag{54}$$

These requirements are necessary but not sufficient for the stau NLSP scenario; indeed, as we have already mentioned, $\widetilde{l}_R\to l\widetilde{G}$ for $l=e,\mu$ can dominate even if Eq. (10) holds, provided that $\sqrt{F}$ is not too large and $\widetilde{l}_R\to l\widetilde{N}_1$ is not open.

As in the slepton co-NLSP scenario of the previous subsection, the discovery prospects are clearest if the decay length $\widetilde{\tau}_1\to\tau\widetilde{G}$ is macroscopic, so that the discovery signal consists of tracks from a heavy $\widetilde{\tau}_1$ and/or kinks due to $\widetilde{\tau}_1$ decays which can be directly observed in the detector [26,34]. In this case, there are no significant physics backgrounds, and the discovery potential is limited only by the total production cross section, the integrated luminosity, and the capabilities of the detectors. In the GMSB models with a stau NLSP, the cross section for $e^+e^-\to\widetilde{\tau}_1\widetilde{\tau}_1$ as a function of $m_{\widetilde{\tau}_1}$ is given to a good approximation by the curves in Fig. 8 with the horizontal axis now interpreted as $m_{\widetilde{\tau}_1}$, and in

---

[5]In the above analysis we did not take into account initial state radiation effects, which diminish total cross sections for both the signal and the backgrounds by up to 10%, and produce slight changes in the shapes of distributions. We do not expect this to significantly affect our conclusions.

particular is not very model dependent. The mixing in the stau (mass)^2 matrix does provide for a small reduction in the $\widetilde{\tau}_1\widetilde{\tau}_1$ cross section compared to that shown, but we have checked that this reduction is at most about 10% in our models. As can therefore be seen from Fig. 8, future LEP 2 runs should be able to discover a long-lived stau NLSP with mass up to close to the kinematic limit, given 300 pb^{-1} or more.

In the following, we therefore concentrate on the more difficult possibility that the $\widetilde{\tau}_1$ decay length is too small to be directly observed. All events will then have an energetic $\tau^+\tau^-$ pair and large missing energy. In the large $\tan\beta$ limit, one has $m_{\widetilde{\tau}_1}\ll m_{\widetilde{e}_R},m_{\widetilde{\mu}_R},m_{\widetilde{N}_1}$ in these models, so that the only discovery signal at LEP 2 is $\tau^+\tau^-\not{E}$. This must be compared to a background from W^+W^- with $W\to\tau\nu$ decays, as given in the previous section. Since the signal events feature E_τ with a flat distribution as in Eqs. (41) and (42), the tau decay length of $\sim 90\ \mu$m$\times E_\tau/m_\tau$ (roughly 1 to 4 mm) may allow for fairly efficient tagging of nonleptonic τ decays. Of course, the W^+W^- background produces taus with a similar energy distribution. Just as discussed in the previous section, the $\widetilde{\tau}_1\widetilde{\tau}_1$ signal is symmetric with respect to $\theta\to\pi-\theta$, while the background is not. Modulo the tau identification problem, Fig. 10 gives an indication of the polar angle distributions of signal and background for $\tau^+\tau^-\not{E}$ events. Extraction of a $\widetilde{\tau}_1\widetilde{\tau}_1$ signal from the background will be considerably more difficult than would be the case for $\widetilde{\mu}_R\widetilde{\mu}_R$ signal in the slepton co-NLSP scenario, and an estimate of the reach will depend quite sensitively on detector capabilities. If the taus are not tagged, one possibility is to look for purely hadronic states with very large missing energy to avoid WW contamination.

For lower $\tan\beta$, the production of $\widetilde{e}_R\widetilde{e}_R$, $\widetilde{\mu}_R\widetilde{\mu}_R$, and/or $\widetilde{N}_1\widetilde{N}_1$ can also be kinematically allowed. For a given model, the $\widetilde{\mu}_R\widetilde{\mu}_R$ cross section is always smaller than that for $\widetilde{\tau}_1\widetilde{\tau}_1$ production, due simply to the kinematic suppression associated with $m_{\widetilde{\mu}_R}>m_{\widetilde{\tau}_1}+m_\tau$. It can of course be read off of Fig. 8, as before. The $\widetilde{e}_R\widetilde{e}_R$ production cross section can be either smaller or larger, due to the interference between graphs with t-channel exchange of neutralinos and s-channel exchange of γ, Z. If $\tan\beta$ does not exceed about 30, these cross sections can add to the signal. Now because of the decays $\widetilde{l}_R\to l\tau\widetilde{\tau}_1$, the signal from $\widetilde{l}_R\widetilde{l}_R$ production is $\tau^+\tau^-(l^+l^-\tau^+\tau^-)\not{E}$, where the leptons in parentheses are much softer. If the leptons are energetic enough to be identified, this signal should have very low backgrounds. It is also possible that both $\widetilde{l}_R\to\widetilde{\tau}_1\tau l$ and $\widetilde{l}_R\to l\widetilde{G}$ have a significant branching fraction, if the former decay is sufficiently kinematically suppressed and $\widetilde{l}_R\to l\widetilde{N}_1$ is not open. The $\widetilde{l}_R\widetilde{l}_R$ production could then lead to the additional signatures $l^+\tau^+(l^-\tau^-)\not{E}$, $l^-\tau^-(l^+\tau^+)\not{E}$, $l^+\tau^-(l^-\tau^+)\not{E}$, $l^-\tau^+(l^+\tau^-)\not{E}$, and, as in the slepton co-NLSP scenario, l^+l^-e.

If $\widetilde{N}_1\widetilde{N}_1$ production is allowed it can provide the dominant signal. In this case, each $\widetilde{N}_1$ can decay predominantly to $\tau\widetilde{\tau}_1$ and then to $\tau^+\tau^-\widetilde{G}$. The final taus from each $\widetilde{\tau}_1$ decay will combine to carry most of the visible energy in each event, and their charges are uncorrelated because of the Majorana nature of $\widetilde{N}_1$. This provides for the striking signatures [37] $\tau^+\tau^+(\tau^-\tau^-)\not{E}$ and $\tau^-\tau^-(\tau^+\tau^+)\not{E}$ and

$\tau^+\tau^-(\tau^+\tau^-)\not{E}$ in the ratio 1:1:2, with the parentheses denoting soft particles as before. As in the case of slepton co-NLSP models, we find that the $\widetilde{N}_1\widetilde{N}_1$ cross section can be up to three times larger than that of $\widetilde{\tau}_1\widetilde{\tau}_1$, despite the requirement $m_{\widetilde{N}_1}>m_{\widetilde{\tau}_1}+m_\tau$. When $\tan\beta$ is not too large, this signal can be the most visible one at LEP 2 for stau NLSP models. If the decays $\widetilde{N}_1\to l\widetilde{l}_R$ are also allowed for $l=e,\mu$, one may obtain the same signatures but with two or four additional soft leptons from the cascade decays of $\widetilde{N}_1$ through $\widetilde{l}_R$. In our stau NLSP models we find that the $\widetilde{N}_1\widetilde{N}_1$ production cross section as a function of $m_{\widetilde{N}_1}$ is still bounded from below (but can be up to 50% smaller than indicated in Fig. 2 in some cases). If $m_{\widetilde{N}_1}\lesssim\sqrt{s}/2-5$ GeV, there should be at least a few events with very energetic same-charge taus and a pair of softer taus with the opposite charge, if more than 300 pb^{-1} is obtained. This is again especially likely to be the discovery signal in models with smaller n and $\tan\beta$ not too large.

D. The neutralino-stau co-NLSP scenario

Finally we consider the case that the lightest neutralino and the lighter stau act effectively as co-NLSP's. This scenario will occur if the conditions of Eq. (12) are satisfied. While it might seem at first that requiring $m_{\widetilde{N}_1}$ and $m_{\widetilde{\tau}_1}$ to be nearly degenerate requires some fine tuning, we find that the region of parameter space where this occurs is actually quite significant. Conditions which are necessary for a viable model (with $m_{\widetilde{N}_1}\gtrsim 70$ GeV) in the neutralino-stau co-NLSP scenario are

$$n=1; \quad 40\ \text{TeV}<\Lambda<80\ \text{TeV}; \quad 15<\tan\beta<40, \text{ or} \tag{55}$$

$$n=2; \quad 20\ \text{TeV}<\Lambda<40\ \text{TeV}; \quad \tan\beta<20, \text{ or} \tag{56}$$

$$n=3; \quad 17\ \text{TeV}<\Lambda<25\ \text{TeV}; \quad \tan\beta<12. \tag{57}$$

Because $\widetilde{N}_1$ and $\widetilde{\tau}_1$ masses are not very different in this scenario, strict exclusion or discovery should be rather straightforward for a given NLSP mass. This is easily understood in terms of the other scenarios we have already studied. We find that in neutralino-stau co-NLSP models, the photino content of $\widetilde{N}_1$ is bounded from below by $\kappa_{1\gamma}>0.35$. Comparing Eqs. (4) and (5) we therefore conclude that if the $\widetilde{N}_1$ decay always occurs outside of the detector, then the $\widetilde{\tau}_1$ decay must also take place over a typically macroscopic distance. If $\widetilde{N}_1\widetilde{N}_1$ production is kinematically allowed, then as in Sec. III A one has a signal $\gamma\gamma\not{E}$ with about a 50% detection efficiency after cuts, as long as the $\widetilde{N}_1$ decay length is not too long. Conversely, if the decay lengths are long, then $\widetilde{\tau}_1\widetilde{\tau}_1$ production leads to a background-free signal with tracks of quasistable $\widetilde{\tau}_1$ observed directly in the detector using the rate of energy loss and/or kinks due to slow decays $\widetilde{\tau}_1\to\tau\widetilde{G}$. In an intermediate regime, one should see both types of events. Note that in any case one need not rely on identifying a $\tau^+\tau^-\not{E}$ (or $l^+l^-\not{E}$) signal against the W^+W^- background to effect discovery. In neutralino-stau co-NLSP models, we find that the $\widetilde{N}_1\widetilde{N}_1$ production cross sections at

TABLE III. The possible signatures at LEP 2 in the four different NLSP scenarios. The notation (1) prompt, (2) within the detector, and (3) outside the detector refers to a NLSP decay such that the decay vertex is (1) close to the interaction region and not measurably displaced, (2) possibly resolvable with a detector, and (3) well outside the detector. In the neutralino NLSP and slepton co-NLSP cases, l stands for e, μ, or τ, in the stau NLSP case l stands for e or μ.

Scenario	Sparticle production	Signal	Comments	
neutralino NLSP	$\widetilde{N}_1\widetilde{N}_1$	$\gamma\gamma\slashed{E}$ displaced γs	$\widetilde{N}_1\to\gamma\widetilde{G}$ decays are	prompt within the detector
	$\widetilde{l}_R^+\widetilde{l}_R^-$	$\gamma\gamma l^+l^-\slashed{E}$ l^+l^-+ displaced γs	(as above)	
slepton co-NLSP	$\widetilde{l}_R^+\widetilde{l}_R^-$	$l^+l^-\slashed{E}^{\mathrm{a}}$ $\widetilde{l}\to l\widetilde{G}$ decay kinks charged $\widetilde{l}$ tracks	$\widetilde{l}\to l\widetilde{G}$ decays are	prompt within the detector outside the detector
	$\widetilde{N}_1\widetilde{N}_1$	$l^+l'^+(l^-l'^-)\slashed{E}$, $l^-l'^-(l^+l'^+)\slashed{E}$, and $l^+l'^-(l^-l'^+)\slashed{E}$	(ll') leptons are soft or undetected	
stau NLSP	$\widetilde{\tau}_1^+\widetilde{\tau}_1^-$	$\tau^+\tau^-\slashed{E}$ $\widetilde{\tau}_1\to\tau\widetilde{G}$ decay kinks charged $\widetilde{\tau}_1$ tracks	$\widetilde{\tau}_1\to\tau\widetilde{G}$ decays are	prompt within the detector outside the detector
	$\widetilde{N}_1\widetilde{N}_1$	$\tau^+\tau^+(\tau^-\tau^-)\slashed{E}$, $\tau^-\tau^-(\tau^+\tau^+)\slashed{E}$, and $\tau^+\tau^-(\tau^+\tau^-)\slashed{E}$	$(\tau\tau)$ leptons are soft or undetected; possibly with 2 or 4 additional soft leptons (e or μ) if $\widetilde{N}_1\to l\widetilde{l}_R$ is open	
	$\widetilde{l}_R^+\widetilde{l}_R^-$	$\tau^+\tau^-(l^+l^-\tau^+\tau^-)\slashed{E}$	$(l^+l^-\tau^+\tau^-)$ leptons are soft or undetected	
neutralino-stau co-NLSP	$\widetilde{N}_1\widetilde{N}_1$, $\widetilde{\tau}_1^+\widetilde{\tau}_1^-$	$\gamma\gamma\slashed{E}$, $\tau^+\tau^-\slashed{E}$ displaced γs and $\widetilde{\tau}_1\to\tau G$ decays kinks charged $\widetilde{\tau}_1$ tracks	NLSP decays are	promp within the detector outside the detector

^aIn the slepton co-NLSP case, the particular $l^+l^-\slashed{E}$ signature which is most likely to be observable is $\mu^+\mu^-\slashed{E}$, as explained in III B.

LEP 2 are bounded from below as in Fig. 2. Likewise Fig. 8 can be used to estimate the $\widetilde{\tau}_1\widetilde{\tau}_1$ production cross section as a function of $m_{\widetilde{\tau}_1}$. This overestimates the actual $\widetilde{\tau}_1\widetilde{\tau}_1$ rate by no more than 10% because of stau mixing effects. When $m_{\widetilde{\tau}_1}$ and $m_{\widetilde{N}_1}$ are more than about 5 GeV below threshold, it cannot be possible for both of these signals to elude detection in future LEP 2 runs.

IV. CONCLUDING REMARKS

In this paper we have studied the implications of gauge-mediated supersymmetry-breaking models for LEP 2 physics. There are four main scenarios for the effective NLSP(s), each with its own predictions for the possible discovery signals. These possibilities also depend on the unknown NLSP decay length, and are summarized in Table III.

In many cases, strict exclusion (or discovery) for a given NLSP mass can be assured given a sufficient beam energy and integrated luminosity. For example, we found that $\sigma(\widetilde{N}_1\widetilde{N}_1)$ is bounded from below (for a given $m_{\widetilde{N}_1}$) in the neutralino NLSP scenario models discussed in Sec. II. We analyzed the backgrounds and found that they can be eliminated with cuts which retain at least 50% of the signal events. This should guarantee discovery of $\widetilde{N}_1$ with masses

up to a few GeV of the kinematic limit in future LEP 2 runs, provided that the $\widetilde{N}_1$ decay length is not too long. As a caveat, we must note that with variations of the model choices we have made, it is quite possible to find smaller cross sections for $\widetilde{N}_1\widetilde{N}_1$ production. For example, there could be additional corrections to the Higgs soft (mass)^2 parameters with an indirect result of smaller values for $|\mu|$ [34]. Similarly, we have investigated some models with unequal nonzero values for the messenger multiplicities $\Sigma_i n_1(i)$, $\Sigma_i n_2(i)$, and $\Sigma_i n_3(i)$ [instead of Eq. (20)], and found that the requirements of correct electroweak symmetry breaking can and do lead to smaller values of $|\mu|/M_2$ in viable neutralino NLSP models. In both cases, one finds that $\widetilde{N}_1$ can have a large Higgsino content, with therefore an arbitrarily small production cross section for a given $m_{\widetilde{N}_1}$ and a very long decay length for $\widetilde{N}_1\to\gamma\widetilde{G}$.

In the slepton co-NLSP scenario, we found that if decays are prompt, the $\mu^+\mu^-\slashed{E}$ signal from $\widetilde{\mu}_R\widetilde{\mu}_R$ production is likely to be the discovery mode. In particular, we found that the $e^+e^-\slashed{E}$ signal from $\widetilde{e}_R\widetilde{e}_R$ production can be highly suppressed by interference effects, and has a comparatively unfavorable polar angle distribution. We also found that it is necessary to employ a different cut on the lepton energies than would be used in the neutralino LSP scenario to sepa-

rate the signal from the WW backgrounds, because of the kinematic characteristics of the decay $\tilde{l} \to l\tilde{G}$ with a nearly massless gravitino. The pair production of $\tilde{N}_1 \tilde{N}_1$ can also lead to spectacular signatures involving two energetic leptons with the same charge (and two softer leptons with the opposite charge), in both the slepton co-NLSP and stau NLSP scenarios. Long slepton lifetimes should lead to a relatively easy discovery from observation of heavy charged particle tracks and/or decay kinks. One of the more difficult scenarios involves a stau which is much lighter than all of the other superpartners and which decays promptly into $\tau\tilde{G}$. In this case the only discovery signal is $\tau^+ \tau^- \not{E}$ with a significant background from WW production.

It should be noted that the signals we have studied are considerably more general than the models outlined in Sec. II. The same scenarios and qualitative features of the signals arise in a much larger class of GMSB models with, for example, different numbers of messenger fields and/or widely different messenger scales. In most cases the discovery of a GMSB signal will be readily distinguishable from the predictions of models with a neutralino LSP. Therefore the variety of different signal possibilities points to the exciting prospect of simultaneously discovering supersymmetry and uncovering some of the most prominent features of the mechanism of supersymmetry breaking.

ACKNOWLEDGMENTS

[1] M. Dine, W. Fischler, and M. Srednicki, Nucl. Phys. **B189**, 575 (1981); S. Dimopoulos and S. Raby, *ibid.* **B192**, 353 (1981); M. Dine and W. Fischler, Phys. Lett. **110B**, 227 (1982); M. Dine and M. Srednicki, Nucl. Phys. **B202**, 238 (1982); M. Dine and W. Fischler, *ibid.* **B204**, 346 (1982); L. Alvarez-Gaumé, M. Claudson, and M. B. Wise, *ibid.* **B207**, 96 (1982); C. R. Nappi and B. A. Ovrut, Phys. Lett. **113B**, 175 (1982); S. Dimopoulos and S. Raby, Nucl. Phys. **B219**, 479 (1983).

[2] M. Dine and A. E. Nelson, Phys. Rev. D **48**, 1277 (1993); M. Dine, A. E. Nelson, and Y. Shirman, *ibid.* **51**, 1362 (1995); M. Dine, A. E. Nelson, Y. Nir, and Y. Shirman, *ibid.* **53**, 2658 (1996).

[3] G. Dvali, G. F. Giudice, and A. Pomarol, Nucl. Phys. **B478**, 31 (1996).

[4] S. Dimopoulos, G. F. Giudice, and A. Pomarol, Phys. Lett. B **389**, 37 (1996).

[5] A. E. Faraggi, Phys. Lett. B **387**, 775 (1996).

[6] M. Dine, Y. Nir, and Y. Shirman, Phys. Rev. D **55**, 1501 (1997).

[7] I. Dasgupta, B. A. Dobrescu, and L. Randall, Nucl. Phys. **B483**, 95 (1997).

[8] S. P. Martin, Phys. Rev. D **55**, 3177 (1997).

[9] A. Riotto, O. Törnkvist, and R. N. Mohapatra, Phys. Lett. B **388**, 599 (1996).

[10] S. Dimopoulos and G. F. Giudice, Phys. Lett. B **393**, 72 (1997).

[11] J. A. Bagger, K. Matchev, D. M. Pierce, and R. Zhang, Phys. Rev. D **55**, 3188 (1997); Phys. Rev. Lett. **78**, 1002 (1997); *ibid.* **78**, 2497(E) (1997).

[12] E. Poppitz and S. P. Trivedi, Phys. Rev. D **55**, 5508 (1997).

[13] P. Ciafaloni and A. Strumia, Report No. hep-ph/9611204 (unpublished); G. Bhattacharyya and A. Romanino, Phys. Rev. D **55**, 7015 (1997).

[14] N. G. Deshpande, B. Dutta, and S. Oh, Phys. Rev. D **56**, 519 (1997).

[15] L. Randall, Report No. hep-ph/9612426 (unpublished).

[16] R. Rattazzi and U. Sarid, Report No. hep-ph/9612464 (unpublished).

[17] N. Haba, N. Maru, and T. Matsuoka, Report No. hep-ph/9612468 (unpublished).

[18] G. Dvali and M. Shifman, Report No. hep-ph/9612490 (unpublished).

[19] N. Arkani-Hamed, J. March-Russell, and H. Murayama, Report No. hep-ph/9701286 (unpublished).

[20] T. Yanagida, Report No. hep-ph/9701394 (unpublished).

[21] R. N. Mohapatra and S. Nandi, Report No. hep-ph/9702291 (unpublished).

[22] S. Raby, Report No. hep-ph/9702299 (unpublished).

[23] F. M. Borzumati, Report No. hep-ph/9702307 (unpublished).

[24] P. Fayet, Phys. Lett. **70B**, 461 (1977); **86B**, 272 (1979); Phys. Lett. B **175**, 471 (1986); in *Unification of the Fundamental Particle Interactions*, edited by S. Ferrara, J. Ellis, and P. van Nieuwenhuizen (Plenum, New York, 1980), p. 587.

[25] N. Cabibbo, G. R. Farrar, and L. Maiani, Phys. Lett. **105B**, 155 (1981); M. K. Gaillard, L. Hall, and I. Hinchliffe, *ibid.* **116B**, 279 (1982); J. Ellis and J. S. Hagelin, *ibid.* **122B**, 303 (1983); D. A. Dicus, S. Nandi, and J. Woodside, Phys. Lett. B **258**, 231 (1991).

[26] S. Dimopoulos, M. Dine, S. Raby, and S. Thomas, Phys. Rev. Lett. **76**, 3494 (1996).

[27] D. R. Stump, M. Wiest, and C. P. Yuan, Phys. Rev. D **54**, 1936 (1996).

[28] S. Ambrosanio, G. L. Kane, G. D. Kribs, S. P. Martin, and S. Mrenna, Phys. Rev. Lett. **76**, 3498 (1996).

[29] S. Dimopoulos, S. Thomas, and J. D. Wells, Phys. Rev. D **54**, 3283 (1996).

[30] S. Ambrosanio, G. L. Kane, G. D. Kribs, S. P. Martin, and S. Mrenna, Phys. Rev. D **54**, 5395 (1996).

[31] K. S. Babu, C. Kolda, and F. Wilczek, Phys. Rev. Lett. **77**, 3070 (1996).

[32] K. Kiers, J. N. Ng, and G. Wu, Phys. Lett. B **381**, 177 (1996).

[33] J. L. Lopez and D. V. Nanopoulos, Phys. Rev. D **55**, 4450 (1997).

[34] S. Dimopoulos, S. Thomas, and J. D. Wells, Nucl. Phys. **B488**, 39 (1997).

[35] H. Baer, M. Brhlik, C.-h. Chen, and X. Tata, Phys. Rev. D **55**, 4463 (1997).

[36] A. Ghosal, A. Kundu, and B. Mukhopadhyaya, Phys. Rev. D **56**, 504 (1997).

[37] D. A. Dicus, B. Dutta, and S. Nandi, Phys. Rev. Lett. **78**, 3055 (1997).

[38] H. E. Haber and G. L. Kane, Phys. Rep. **117**, 75 (1985); J. F. Gunion and H. E. Haber, Nucl. Phys. **B272**, 1 (1986); **B402**, 567(E) (1993).

[39] S. Park, in *10th Topical Workshop on Proton–Anti-proton Collider Physics*, edited by Rajendran Raja and John Yoh (AIP, New York, 1995).

[40] CDF Collaboration, D. Toback, spokesperson, Report No. FERMILAB-CONF-96-240-E, 1996 (unpublished).

[41] D0 Collaboration, S. Abachi *et al.*, Phys. Rev. Lett. **78**, 2070 (1997).

[42] H. Pagels and J. R. Primack, Phys. Rev. Lett. **48**, 223 (1982); T. Moroi, H. Murayama, and M. Yamaguchi, Phys. Lett. B **303**, 289 (1993); S. Borgani, A. Masiero, and M. Yamaguchi, *ibid.* **386**, 189 (1996); M. Kawasaki, N. Sugiyama, and T. Yanagida, Report No. hep-ph/9607273 (unpublished); T. Gherghetta, Nucl. Phys. **B485**, 25 (1997); A. de Gouvêa, T. Moroi, and H. Murayama, Phys. Rev. D **56**, 1281 (1997).

[43] M. Chen, C. Dionisi, M. Martinez, and X. Tata, Phys. Rep. **159**, 201 (1988).

[44] H. Baer, M. Brhlik, R. Munroe, and X. Tata, Phys. Rev. D **52**, 5031 (1995).

[45] The Standard Model Process Group, F. Boudjema *et al.*, *Proceedings of the Workshop ''Physics at LEP2,''* edited by G. Altarelli, T. Sjöstrand, and F. Zwirner, CERN Report No. 96-01, 1996 (unpublished), Vol. 1, p. 207.

[46] E. E. Boos, M. N. Dubinin, V. A. Ilin, A. E. Pukhov, and V. I. Savrin, Report No. hep-ph/9503280 (unpublished), and references therein.

[47] S. Ambrosanio, G. L. Kane, G. D. Kribs, S. P. Martin, and S. Mrenna, Phys. Rev. D **55**, 1372 (1997).

[48] ALEPH Collaboration, Phys. Lett. B **384**, 427 (1996).

[49] DELPHI Collaboration, Report No. CERN-PPE/96-188 (unpublished).

[50] David D. Stuart (private communication).

[51] ALEPH Collaboration, Phys. Lett. B **373**, 246 (1996); DELPHI Collaboration, *ibid.* **387**, 651 (1996); L3 Collaboration, *ibid.* **377**, 289 (1996); OPAL Collaboration, Report No. CERN-PPE/96-096 (unpublished).

[52] S. Kawabata, Comput. Phys. Commun. **41**, 127 (1986); S. Kawabata and T. Kaneko, *ibid.* **48**, 353 (1988).